AD-779 907

MOLDING OF ORIENTED SHORT FIBER COMPOSITES. III. RATE EFFECTS ON FIBER ALIGNMENT IN CONVERGENT CHANNELS

L. A. Goettler

Monsanto Research Corporation

Prepared for:

Office of Naval Research
Advanced Research Projects Agency

May 1974

DISTRIBUTED BY:

NTIS

National Technical Information Service
U. S. DEPARTMENT OF COMMERCE
5285 Port Royal Road, Springfield Va. 22151

HPC 72-150 ITEM A002

MOLDING OF ORIENTED SHORT FIBER COMPOSITES
III. RATE EFFECTS ON FIBER ALIGNMENT IN CONVERGENT CHANNELS

by

L. A. GOETTLER
Monsanto Company

DDC
RECEIVED
JUN 7 1974
C

May 1974

Monsanto/Washington University Association
High Performance Composites Program
Sponsored by ONR and ARPA
Contract No. N00014-67-C-0218, ARPA Order 876

Approved for Public Release; Distribution Unlimited

Monsanto Research Corporation
800 N. Lindbergh Blvd.
St. Louis, Missouri 63166

ib

AD 779907

Security Classification

DOCUMENT CONTROL DATA - R & D

(Security classification of title, body of abstract and indexing annotation must be entered when the overall report is classified)

1. ORIGINATING ACTIVITY *(Corporate author)* Monsanto Research Corp.	2a. REPORT SECURITY CLASSIFICATION Unclassified 2b. GROUP

3. REPORT TITLE

Molding of Oriented Short Fiber Composites
III. Rate Effects on Fiber Alignment in Convergent Channels

4. DESCRIPTIVE NOTES *(Type of report and inclusive dates)*

5. AUTHOR(S) *(First name, middle initial, last name)*

L. A. Goettler

6. REPORT DATE May 1974	7a. TOTAL NO. OF PAGES 68	7b. NO. OF REFS 17
8a. CONTRACT OR GRANT NO. N00014-67-C-0218 b. PROJECT NO. c. d.	9a. ORIGINATOR'S REPORT NUMBER(S) HPC 72-150 9b. OTHER REPORT NO(S) *(Any other numbers that may be assigned this report)*	

10. DISTRIBUTION STATEMENT

Approved for public release; distribution unlimited

11. SUPPLEMENTARY NOTES	12. SPONSORING MILITARY ACTIVITY Office of Naval Research Washington, D. C.

13. ABSTRACT

In an extension of the experiments performed on the compacted flow of a glass fiber-filled epoxy resin through a conical converging channel under a high pressure, this study examines the orientability of the fibers as the suspension flows into an empty mold cavity. The tensile properties of molded rods of 1/4" to 1/2" diameter reflect the level of orientation produced.

Both the fiber orientability and the resulting orientation distribution depend strongly on the rate of elongation. The molded-in orientation distribution is also determined by the extent of convergence. Convergence angle, viscosity, and fiber length are secondary variables. The results indicate that fibers can be oriented to within 20° of the flow axis by this technique in order to maximize mechanical performance. The anomalous dependence on the rate of elongation is thought to result from the high voidage in the material during flow.

Reproduced by
NATIONAL TECHNICAL
INFORMATION SERVICE
U S Department of Commerce
Springfield VA 22151

DD FORM 1 NOV 65 1473 (PAGE 1)

S/N 0101-807-6801

Security Classification

Security Classification

14 KEY WORDS	LINK A ROLE	LINK A WT	LINK B ROLE	LINK B WT	LINK C ROLE	LINK C WT
plunger molding						
transfer molding						
flow						
flow rate						
elongational flow						
fiber orientation						
composite						
epoxy						
fiberglass						
tensile modulus						
tensile strength						
convergence flow						

DD FORM 1 NOV 65 1473 (BACK)
(PAGE 2)

ia

Security Classification

FOREWORD

The research reported herein was conducted by the staff of Monsanto/Washington University Association under the sponsorship of the Advanced Research Projects Agency, Department of Defense, through a contract with the Office of Naval Research, N00014-67-C-0218 (formerly N00014-66-C-0045), ARPA Order No. 876, ONR contract authority NR 356-484/4-13-66, entitled, "Development of High Performance Composites."

The prime contractor is Monsanto Research Corporation. The Program Manager is Dr. Rolf Buchdahl (Phone 314-694-4721).

The contract is funded for $7,000,000 and expires 30 June, 1974.

Molding of Oriented Short Fiber Composites

III. Rate Effects on Fiber Alignment in Convergent Channels

by

L. A. Goettler

ABSTRACT

In an extension of the experiments performed on the compacted flow of a glass fiber-filled epoxy resin through a conical converging channel under a high pressure, this study examines the orientability of the fibers as the suspension flows into an empty mold cavity. The tensile properties of molded rods of 1/4" to 1/2" diameter reflect the level of orientation produced.

Both the fiber orientability and the resulting orientation distribution depend strongly on the rate of elongation. The molded-in orientation distribution is also determined by the extent of convergence. Convergence angle, viscosity, and fiber length are secondary variables. The results indicate that fibers can be oriented to within 20° of the flow axis by this technique in order to maximize mechanical performance. The anomalous dependence on the rate of elongation is thought to result from the high voidage in the material during flow.

This research was supported by the Advanced Research Projects Agency of the Department of Defense and was monitored by the Office of Naval Research under Contract No. N00014-67-C-0218.

Molding of Oriented Short Fiber Composites

III. Rate Effects on Fiber Alignment in Convergent Channels

by

L. A. Goettler

A polymer melt containing short reinforcing fibers constitutes an anisotropic fluid that orients in response to the hydrodynamic forces induced by flow deformation. The most prominent mechanism for effecting a change in orientation direction is that of uniaxial extension. This commonly occurs in the stretching of a material, from which it appears intuitive that the fibers will align along the direction of stretch. Their rate of rotation in an elongational flow field can be derived from the mechanics of dilute suspensions of ellipsoids, as given by (1), by considering the fibers of aspect ratio 25 to 500 to represent a limiting case of high ellipticity. Alternately, an equivalent expression can be derived from considerations of invariance in the constitutive relationships for anisotropic fluids (2). In either case, the rate of orientation change is given by

$$\dot{\theta}_1 = -\frac{3}{4}\lambda\left(\frac{dv_1}{dx_1}\right)\sin 2\theta_1 \tag{1}$$

$$\dot{\phi}_1 = 0 \tag{2}$$

where θ_1 is the polar angle of the fiber axis in a spherical coordinate system whose coordinate axis is in the direction of stretch.

ϕ_1 is the corresponding longitude.

$\frac{dv_1}{dx_1}$ is the axial velocity gradient at the fiber center.

λ is an orientability parameter.

In the case of fiber suspensions in a matrix resin of viscosity less than 500 poise, like a B-staged epoxy, conduit flow is lubricated by a thin layer of resin at the wall so that the central plug of fibers that encompasses most of the channel cross-section does not experience any shear (3). Axial flow through a conical converging channel then becomes an elongational flow in which the elongation rate is a function of axial position alone:

$$\dot{\varepsilon}_{11} = \frac{dv_1}{dx_1} = \frac{Q}{\pi x_1^{\,3}(1 - \cos\alpha)} \tag{3}$$

where Q is the volumetric flow rate.

Substitution of Equation (3) into (1) followed by integration along a streamline then gives

$$\frac{\tan\theta_1}{\tan\theta_1^{\circ}} = \left(\frac{x_1}{x_1^{\circ}}\right)^{3\lambda} = \left(\frac{A}{A^{\circ}}\right)^{\frac{3}{2}\lambda} \tag{4}$$

where A is the area of a spherical surface of radius x_1 centered at the vertex of the cone and subtended by the walls of the conical channel. For all practical purposes it is equal to the cross-sectional area of the channel at x_1. This equation applies either to the motion of a single fiber or to the instantaneous collective distribution of the orientations of all fibers lying along a streamline. It is used in the latter sense in this paper. Details are given by Goettler (4).

The channel geometry to which this equation is applied is shown in Figure 1. The coordinate angles are also identified in this diagram. Flow is from left to right. Further upstream, and not shown, is a small entrance gate preceded by a runner system that leads to a plunger chamber. It has been observed that when angles measured along a streamline are plotted against axial position in the cone for flows of dense materials, Equation (4) is obeyed. This result also implies that the flow is sufficiently steady that all fiber orientations measured along the streamline correspond to the same initial state θ_1°. These experiments in which an epoxy/glass fiber molding compound is caused to flow under pressure in a transfer mold are fully documented elsewhere (4). Since the same materials, geometry, and analyses are used in the work reported here, the details will not be repeated.

When not compressed, a 40 v/o suspension of 1/8" long fibers shows a large amount of voidage due to the high aspect ratio and stiffness of such fibers. For a three-dimensionally random material, the maximum fiber content , exclusive of voids, for packing of the fibers without breaking is about 30 v/o. This value would be increased if the fibers are bundled or show some alignment. Injection molding through small gates at moderate to high rates tends to expand the molding compound to an even lower bulk density until it is compacted in the mold.

At lower fiber contents of 20-25 v/o, the molding compounds contain much fewer voids even when not under pressure and tend to flow more in the manner of a liquid. Their orientability is described by the model with constant λ even when flowing into an empty cavity. The pressure drop induced by the flow itself is probably sufficient to cause whatever voids are present to close up.

However, when an empty mold cavity is injected with molding compound of a higher content of fibers (40 v/o), the model represented by Equation (4) is not obeyed. This may be due to the high porosity. The type of variation in the slope, λ, of a plot of ln tan θ_1 vs ln x_1 is shown in Figure 2. The planar angle ϕ_3 used in that plot in place of θ_1 is explained in (4) to be a constant factor of θ_1. ϕ_3 is the planar angle between the fibers and the streamline that was measured from polished

axial sections cut through the moldings. It represents the local mean orientation of a close grouping of fibers. The dashed line in the figure shows how an effective orientability, λ_{eff}, can be fitted by a least squares analysis to the data.

The purpose of this work is to study the variation in λ_{eff}, hereafter simply called λ, as a function of material and flow conditions for those substances investigated in which it is not a true material constant. Causes for this anomalous behavior and limitations on λ will also be treated. Since, under the proper conditions, the orientability may increase to very high levels, the optimum tensile properties of molded rods are compared with those obtained by other orientation techniques.

Definition of variables.

Equation (4) predicts that the orientation change depends upon the change in cross-sectional area and upon the orientability parameter, λ. This study will center on the effect of elongation rate, $\dot{\varepsilon}_{11}$ as a function of the volumetric flow rate, Q, the polar angle of the cone surface, α, and the axial position in the cone, x_1. A typical variation in $\dot{\varepsilon}_{11}$ with x_1 is shown in Figure 3 where it is indicated that $\dot{\varepsilon}_{11}$ changes rapidly to extremely high values in the vicinity of the small exit of the cone. For purposes of correlation with λ, it is necessary to define an average $\dot{\varepsilon}_{11}$, denoted $\bar{\dot{\varepsilon}}_{11}$, for the cone.

$$\bar{\dot{\varepsilon}}_{11} = \frac{1}{x_{1,in} - x_{1,out}} \int_{x_{1,out}}^{x_{1,in}} \dot{\varepsilon}_{11}\, dx \qquad (5)$$

$$= \frac{1}{2} \left(\dot{\varepsilon}_{11}\right)_{in} \frac{x_{1,in}}{x_{1,out}} \left(1 + \frac{x_{1,in}}{x_{1,out}}\right) \qquad (6)$$

The average elongation rate is then a function of Q, α, and d, the cone outlet or attached rod diameter. Values are given in Table I.

The material variables investigated in this portion of the study include the individual fiber aspect ratio, ℓ/d_f, and the initial bundle aspect ratio, ℓ/d_b. Although the bundles are partially opened by fluid deformation during flow, some integrity remains, which may influence both the observed orientability, λ, and the mechanical properties of the molded rods. A complete listing of the parameters affecting the orientation is given in reference (4), of which this work is a continuation.

The rods of diameters 1/2", 3/8" and 1/4" were filled directly from the outlet of the conical converging section, as shown in Figure 1. Because of the low viscosity (< 5,000 poise) of the epoxy molding compounds, the orientation pattern produced in the cone was not altered by shear flow in the rod. Consequently, except for hydrodynamic effects near the juncture of the two, the tensile properties exhibited by the rod should correspond to the orientability of the material measured in the cone.

In these composites, Young's modulus is a strong function of the fiber orientation and shows little dependence on other aspects of composite structure. The ultimate properties of moldings in which the fibers are preferentially oriented into the stress direction are also predominantly determined by the degree of fiber alignment. However, when orientation is more adverse, void content, fiber wet-out and fiber dispersion become critical (5). Tensile strength, modulus, and ultimate elongation were measured by mounting the rods in holding blocks and pulling them on an Instron testing machine. Tensile strain was measured by an extensometer clipped to the sample surface.

The orientation produced by the cone depends upon the distribution of fiber angles entering from the large upstream section. That orientation is nominally transverse in the center, but it is turned into the direction of flow along the wall. The average level of orientation in the rods predicted from measured λ-values is based upon the use of an average upstream orientation angle to represent this distribution. This average θ_1° was found to be approximately 77° in all of the experiments. In the determination of the λ-values, on the other hand, the orientability was measured locally along single streamlines placed midway between the axis and the wall of the cone.

Wall Effect

If the center of mass of a fiber lies closer than half the fiber length to a solid surface, its orientation is biased by

physical interaction directly with the wall. The fiber will not be allowed to assume orientation angles with the wall surface that are greater than a value depending on the distance of the centroid from the wall. Orientation consequently tends to become more "longitudinal," i.e., following the walls of the channel. This is enhanced by locally high shearing stresses in the suspension near the wall. Even when the fiber is further removed from the solid surface, some effects may still be transmitted through the oriented fibers that form a boundary layer in the fluid close to the wall. However, such wall effects are negligible when applied to overall orientation obtained in the moldings under study, as long as the channel diameter exceeds the fiber length.

In addition to the evidence presented in (4), Figure 4 shows a plot of two representations of the planar angle ϕ_3 at the downstream end of the cone. The value plotted on the ordinate was extrapolated from a regression analysis of the angle measurements as a function of axial position along a streamline that lies 50% of the radial distance from the axis to the cone surface. Actual measured values of the downstream angle from the same samples are plotted as the abscissa. The different data points in the figure correspond to variations in the flow rate that caused a changing degree of perfection in the orientation. Since the wall effect should be greater at the smaller downstream end of the cone, an agreement between the extrapolated and measured angles would be taken to indicate

the absence of a wall effect. The 45° line in this figure shows that such equality is indeed very nearly obtained when the degree of longitudinal orientation is high (ϕ_3 small). The points at larger ϕ_3 in Figure 4 corresponds to samples made with higher flow rates and an accompanying lower orientability. Actual orientation becomes poorer than that predicted by extrapolation of the axial data. Although this is unquestionably a flow effect, the observations are contrary to the influence of the wall.

Other evidence for the absence of a wall effect is the observed drop in rod stiffness below that predicted on the basis of the measured orientability of the suspension as rod diameter decreases. This behavior has been observed (4) for 1/8" fibers which are always smaller in length than the rod diameters investigated. Because in smaller rods the area of wall influence is a much larger proportion of the total cross-sectional area, the operation of a wall effect would be expected to cause an increase rather than the observed decrease in the measured stiffness for small rods.

Correlation of Elongation Rate Effects.

As was mentioned earlier and shown by Equations (3) and (6), the average elongation rate in the conical converging section is a function of the flow rate Q, the angle of convergence α, and the diameter of the cone outlet d, which is also the diameter of the molded rod attached to the cone. The effective values of the orientability parameter λ were measured as described earlier

for the flow of a 40 v/o suspension of 1/8" CS308A glass fibers in an epoxy matrix. Two cone angles of 6° and 22-1/2° were employed. Average elongation rates are obtained from Table I. The data plotted in Figure 5 show that λ increases for small increasing elongation rates, passes through a maximum at a critical elongation rate, denoted by $\dot{\varepsilon}^*_{11}$, at 0.36 seconds^{-1} and decreases at elongation rates above this critical value. The data for the two cone angles are seen to fall into coincidence on this plot, showing that the separate effects of flow rate and cone angle can be combined into a single parameter: elongation rate. It should be noted that, unlike the case treated in reference (4) for flow under a compaction pressure, the orientability in this case can attain values larger than unity at the optimum point.

The corresponding modulus measurements on 3/8" diameter molded rods are shown as a function of the average elongation rate in Figure 6. Single data points on this and the preceding figure refer to individual moldings, except those with range marks showing the magnitude of the standard deviation of the mean of several values at that point. The overall reproducibility of the stiffness measurements for rods molded under similar conditions is 0.21×10^6 psi. Again it can be seen that the data points on the 6° and 22-1/2° cones are in agreement when plotted on the basis of the average elongation rate in the cone. The dashed curve in the figure represents the best fit to the experimental data.

The solid curve represents the stiffness that would be predicted from the model given in Equation (4) utilizing the measured values of λ that have previously been presented in Figure 5. An upstream angle θ_1° of 77° is used to calculate the average angle at the cone exit, or in the rod, which is then converted into a predicted average rod stiffness according to a previously determined correlation of experimental data on various transfer moldings that is given by Figure 7.

Both the predicted and experimental curves pass through a maximum at the same critical elongation rate of 0.36 seconds^{-1} that appears in Figure 5. The experimental and theoretical curves are in agreement at an average elongation rate of .15 seconds^{-1}, which was the lowest rate studied. The two curves are again in coincidence at moderate elongation rates ranging from 1.5 to 15 seconds^{-1}. However, in the decade of rates between .15 and 1.5 seconds^{-1} there is a large disparity between the predicted and experimental moduli.

In this range, which contains the optimum elongation rate, the orientability λ is very large, which results in the high predicted modulus of 4.5×10^6 psi. However, for reasons relating to the stability of the flow, which will be discussed later, the actual orientation distribution in the rod is restrained from reaching the high predicted values. At the very high elongation rates in excess of 15 seconds^{-1} an unexpected jump is observed in the measured modulus of the rod. This anomaly is not observed in the measurement of the orientation parameter λ. It can be attributed to a stabilizing effect in the flow which will be discussed later.

The variations in rod modulus are opposite to effects attributable to the small variations observed in the upstream angle θ_1°. In general, rate dependence of the orientability λ is the overriding effect determining the mechanical properties of the molded rods.

The tensile strength of the molded rods shows a similar dependence upon the elongation rate. However, in this case, the optimum rate occurs in a value about 4 times higher than that observed for the stiffness and the orientability parameter. This can be attributed to the dependence of strength, an ultimate property, upon factors other than the orientation of the fibers. For example, the dispersion of the fibers continues to increase with increasing rate of deformation, and this is beneficial to the strength. The tensile strength varies from a low value of 14,000 psi at a rather high elongation rate of 7 seconds^{-1} to a high value of 28,000 psi at the optimum elongation rate for strength of 1.5 seconds^{-1}. The standard deviation of the mean for tensile strength measurements is about 1500 psi.

The determinations of the orientability parameter λ are replotted in Figure 8 to show the range of viscosity levels; as in the case of experiments with flow under a compaction pressure (4) a normalized apparent Newtonian viscosity is used. In the study of flow into an empty mold cavity, the ΔP over the entire path from ram to vent can be measured during the flow. Since P_{vent} is approximately equal to 0, we take $\eta = k \frac{P_{ram}}{Q}$. The total viscosity changes caused by variations in the degree of reaction of the epoxy matrix in the

B-stage range over a factor of 67. However, because most of the data were taken at a constant ram pressure, there is a correlation between the two variables of flow rate and viscosity. Consequently, the viscosity range covered at a given flow rate is much smaller than the total range. This is shown in Figure 8. However, there is sufficient overlap of runs made at different viscosity levels to indicate that the behavior of λ is independent of viscosity and is rather a true function of the flow rate or rate of elongation. Although not reported here, the measured rod stiffness shows a similar independence of viscosity. This in in line with the results obtained with flow under pressure (4). λ in that case was a constant independent of Q, but it was also independent of viscosity over a 25 fold range.

In the case of a 90° entrance angle, α, a dead region will form in the corners at the point of cross-section reduction. The flowing fluid will then experience a more gently converging natural channel that is formed by the stagnant regions. An effective convergence angle was estimated at about 50° in the samples, but it likely changes with the fill rate and rheological properties of the molding compound. (A value of 30° was derived from pressure drop-convergence angle correlations by Stankoi (6) for polyester premix.) Because of this, it is not possible to calculate an elongation rate; the rod stiffness can only be correlated against the volumetric rate of flow through the constriction, as in Figure 9. When multiple measurements at fixed flow rate were available, the standard deviation of the mean was indicated by a bracketed vertical line segment.

There are several important observations from this graph. Two overlapping branches result. The flow phenomenon causing this separation probably has a stochastic nature, rather than being a deterministic function of the flow or elongation rate. The lower branch corresponds to the curves discussed previously for 6° and 22.5° entrance angles, and consequently correlates with predictions of stiffness from the measured λ. For example, with an effective 50° entrance angle at high flow rates, those data points can be translated approximately into terms of an average elongational strain rate and compared with the data from Figure 6 in Table 2. This good agreement shows that the lower curve represents the alignment resulting from fiber rotation in the converging flow. It was not obtained at lower flow rates with the 90° entrance angle, possibly because of a change in the character of the flow or a different convergence angle.

The upper branch in Figure 9 corresponds with the two isolated points at high elongation rate for the tapered cones in Figure 6. These results closely coincide in both stiffness and elongation rates when compared on the basis of a 50° effective angle for the 90° entrance. The high level of stiffness results from an unusually smooth flow that occurs at very high rates of elongation. This will be discussed later.

The effect of area reduction ration $A°/A$, or final rod diameter, on rod stiffness and strength is given in Table 3 for the 90° geometry. In this case the degree of alignment is independent of area reduction ratio at the same value of Q.

The strength data for the 3/8" rod are represented as a function of flow rate, Q, in Figure 10. The same two branches that were observed in the stiffness correlation again occur. As in the case for $\alpha = 6°$, the maxima in the strength curve occur for higher values of Q or $\bar{\dot{\varepsilon}}_{11}$ than for stiffness. The ultimate elongation of the samples was approximately constant at 1.0%.

It has been seen that the data for cones of different angle can be superimposed by correlating as a function of the average elongational strain rate in the cone, $\bar{\dot{\varepsilon}}_{11}$. Similarly, the data in Figures 11 and 12 in conjunction with Figure 6 show that $\bar{\dot{\varepsilon}}_{11}$ can be used as the correlating parameter when the rod diameter (or cone exit diameter) is changed, keeping the cone angle and flow rate constant. In each case, the rod stiffness can be predicted from the single plot of $\lambda(\bar{\dot{\varepsilon}}_{11})$ (Figure 5) by using the experimental relationship of sample stiffness to average axial angle (Figure 7) that was mentioned previously. These stiffness predictions are different because the various rods represent different area reduction ratios $\left(\frac{A_o}{A}\right)$ in Equation (4).

In each case, agreement of the experimental data with the predictions is indicated at both low and at moderately high elongation rates, but there is a wide discrepancy of 20-30 percent at the optimum point, $\bar{\dot{\varepsilon}}^*_{11}$. It appears that $\bar{\dot{\varepsilon}}^*_{11} = 0.36\ \text{sec}^{-1}$ and is independent of $\frac{A_o}{A}$. Table 4 compares the actual orientation (calculated from the measured elastic modulus of the rod) to that predicted from the measured orientability, λ, and an initial

angle θ_1° of 77°. In the small (1/4") diameter rods, the deviation of attained orientation from that anticipated extends over a wide range, exceeding one decade of extension rate about the optimum point. For such large area reduction ratios a high degree of orientation is predicted over a larger range of λ and hence of $\bar{\varepsilon}_{11}$ than for the larger channels. It must be concluded from Table 4 that alignments better than an average angle of about 20° just are not possible in practice. The effect of reaching a limiting orientation occurs both in approaching the optimum flow rate and decreasing the channel diameter. In the case of decreasing rod diameter, the mechanical properties may even degenerate. This is shown more clearly in Table 5 where the comparison for different area reduction ratios is based on mechanical properties rather than angles.

For the 1/4" diameter rod, the tensile strength showed a small general decline from 23,000 to 16,000 psi over the range of elongation rates of 1. to 200 sec^{-1}. The average of the measured values was 20,300 psi. This decline roughly parallels the behavior of the elastic modulus that was indicated in Figure 11. Strengths of the 1/2" diameter rods pass through a maximum of 20,000 psi at an average elongation rate slightly higher than the 0.36 sec^{-1} observed for modulus, as shown in the insert in Figure 12. This figure also demonstrates a lack of dependence on gate diameter, a result also found in the previous study (4) with flow under pressure. The ultimate elongation for these samples ranged between 0.6 and 0.9%.

Fiber Length

When the fiber length is increased to 1/4", the fiber orientability, λ, shows considerably less variation with elongation rate than in the case of 1/8" fibers. This is demonstrated in Figure 13. At $\bar{\varepsilon}^*_{11}$, the peak value of λ is only 0.86, which is 25 percent lower than that obtained with 1/8" fibers. The diminished variation in λ for the 1/4" fibers is reflected in the mechanical properties of the molded rods, which generally show no significant dependence on flow rate.

An exception was observed for the 1/2" rod ($A°/A = 6.25$), where the characteristic peak in E occurred at about .36 sec^{-1} elongation rate. This is the same critical value of $\bar{\varepsilon}_{11}$ that was measured for the 1/8" fibers. The modulus and tensile strength data for the 1/4" fibers are plotted in Figure 14. Over a large part of the range at the lower elongation rates there is no apparent variation with $\bar{\varepsilon}_{11}$, because λ is essentially constant in that region. As before, the tensile strength peaks out (at 21,000 psi) at a slightly higher value of the elongation rate. The ultimate elongation is constant at .82%. The change in properties near $\bar{\varepsilon}^*_{11}$ may have been masked in the cases of the other rods molded with 1/4" fibers by imprecision in the data.

According to the peak λ value of 0.86 read from Figure 13, the predicted rod modulus at .36 sec^{-1}, the critical elongational rate, should be 3.2×10^6 psi for the 1/2" rod. That is almost exactly the value appearing in Figure 14. This calculation uses an entrance fiber angle, θ°_1 of 77°, as with the 1/8" fibers. On the other hand, the average measured elastic modulus

for 3/8" diameter rods ($A^{\circ}/A = 11.1$) is $3.12 \pm .07 \times 10^{6}$ psi at a fiber content of 44 v/o. This translates to 2.86×10^{-6} psi at the standard 40 v/o loading. The corresponding λ of 0.61 is almost equal to the average value of 0.63 measured over the same range of deformation rates. This result substantiates the previous observation (for 1/8" fibers) that, when the degree of alignment is limited by a low λ value, and/or a small area reduction ratio, the measured stiffness of molded rods can agree closely with that predicted from the orientation model. The ultimate tensile strength and elongation of these moldings are 27,600 psi and 1.1%, respectively.

The shorter milled glass fibers show a monotonic increase in orientability with increasing elongation rate. The attendant increase in rod modulus is plotted along with λ in Figure 15. Tensile strength increases slightly from 8,000 to 9,000 psi with increasing elongation rate over this range. Reasons for the absence of an extremum with this material are presented under Discussion. Under all conditions, the properties of rods molded from milled fibers are lower than when longer chopped fibers are used. Not only do the shorter fibers align more poorly, as evidenced by their considerably lower λ's, but even in a perfectly aligned composite they would carry only a small portion of the load because of their low aspect ratio.

Bundle aspect ratio.

An additional size parameter that was not considered in (4) is the aspect ratio of the fiber bundles that are incorporated into the molding compound. Johns Manville chopped glass strand

is available in two types which supposedly employ the same binder and differ only in the number of fiber ends. Type 308 has 120 filaments per strand, while 308A has 240. The chopped strand is coated with a high integrity binder that contains a silane coupling agent and is epoxy compatible. Microscopic examination of the transfer moldings shows that the degree to which the bundles of fibers are opened up during the molding operation depends upon the deformational energy expended, but that in no case is the bundle completely annihilated. A typical section is shown in Figure 16. Consequently, the initial bundle aspect ratio may have some effect on the fiber orientability when the other geometric variables are held constant.

A comparison of the moduli of molded 3/8" rods using a 6° converging conical nozzle is shown in Table 6. The sample standard deviation indicates that there is no significant difference between the orientation behavior of the two materials. The ultimate tensile properties, which are also included in the table, support this conclusion.

Discussion

1. Property comparisons

A summary of the molded rod tensile properties is shown in Table 7. The optimum fiber length is a function of elongation rate. If the flow rate and geometry can be manipulated to keep $\dot{\varepsilon}_{11}$ at its critical value of 0.30 sec^{-1}, the very high λ for 1/8" fibers at this point makes them the preferred length. Tensile

strength and modulus equal or excel the properties obtained with 1/4" fiber because the higher λ allows the 1/8" fibers to orient into a higher degree of uniaxial alignment.

This result supports the experimental findings of Hoffman and Fiala (7) working with diallyl phthalate molding compounds. In a later work Hoffman and Vellturo (8) contend that the optimum mechanical strength, equalling or exceeding that obtained from 1/2" fibers in transfer molding, results from the flowability, strand integrity and ability to orient. The latter factor indicates a high value of λ, as we find at F^*_{11}; their conjecture that screw processing is necessary to obtain highly oriented moldings, however, is shown to be too restrictive by the results of this study. Indeed, in properly designed convergent geometries, very high tensile properties can be obtained in plunger moldings.

At higher elongation rates, where the λ's for 1/8" and 1/4" fibers are identical (see Figure 13) the 1/4" fibers produce superior properties. In the case of the 1/4" rod, this could be due to a physical interaction with the wall that operates to preferentially orient the longer 1/4" fibers into the direction of flow. In a 1/4" rod, the only 1/4" fibers that can occupy a completely transverse position are those which lie on a diameter. On the other hand, 1/8" fibers in 75% of the contained rod volume could orient in that extreme position. More generally, the flow with 1/4" fibers could possibly be more stable, or perhaps the enhancement in mechanical properties could just depend on

structural parameters other than orientation.

The optimum degree of alignment and tensile properties obtained by controlled transfer molding are compared with similar composites prepared by other techniques in Table 8. Controlled transfer molding and compression molding of extruded rod prepregs are similar in that fiber orientation is obtained by a converging flow in each case. The first two entries of the table show that similar properties result. The best possible average polar angle of fibers about the axis is seen to be about 20°. Phenomena that contribute to this limitation are discussed below. For comparison, the very low property levels obtained in a conventional molding geometry utilizing a small gate at the end of a test bar are presented as the third entry. Tensile strength is particularly limited by the transverse fibers in the centers of these moldings.

Higher degrees of orientation can be obtained either with more sophisticated flow equipment, as in the ERDE process, or by meticulous laboratory methods. The latter involve the production of highly elongated grains of individually coated fibers, either by fiber suspension in a Couette flow field, or by hand-stretching a mass of fibers that has been impregnated with resin. The B-staged grains are then hand laid into cavities and compression molded. These techniques produce high property levels, with average angles at about 10°, but are not amenable to large scale production. The ERDE process is used to produce a commercial graphite fiber/epoxy prepreg. It employs a special moving trough to deposit short fibers suspended in a low viscosity

solvent into an aligned mat. The flow field at the trough exit is a type of elongational flow. Tensile data are available only for compression moldings of graphite fiber prepregs. Taking into account the differential in stiffness between glass and graphite fibers, the reported properties in Table 8 indicate an improvement over the extrusions and transfer moldings that is slight in modulus, but significant in tensile strength.

2. Orientation behavior

At the same fiber content (40 v/o), higher orientabilities (up to $\lambda = 1.2$ for 1/8 fibers) are measured in this work than can be realized when the material is compacted under several thousand psi before flow occurs. Then the measured λ is only 0.47. When molding into an empty mold cavity, the void content in the molding compound is high. By stopping the flow when the cavity is only part filled, the noncompacted material can be cured and then removed for examination. The high void contents exceeding 10% found in these "short shots" compare with 2-3% in the completed moldings. Such a high voidage could give an increased mobility to the fibers and hence the higher value of λ. This would be similar to the effects of free volume on a molecular level.

Other evidence exists to support the hypothesis that it is the rotational mobility of the fibers that determines the value of λ. The peak λ of 0.86 read from Figure 13 for 1/4" fibers

is 26% below the peak for the shorter 1/8" fibers. Because of their larger length, they interact and tend to bend and tangle to a higher degree; hence, they have a lower mobility. If fiber length is decreased too much, however, λ will decrease to low values, as in the case of the milled fibers. When fibers are too short the hydrodynamic forces causing the fiber rotation are not fully developed. The opposing requirements of a sufficiently long fiber to realize the maximum forces and a sufficiently short fiber to minimize fiber interactions are compromised in the optimum fiber length of 1/8".

In (4) it was found that, with compacted material, a decrease in the fiber content causes an increase in λ. The orientability increases from 0.47 to 0.75 as the concentration of fibers is halved to 20 v/o. At the lower concentration, there is a lower degree of fiber interaction, resulting in a higher mobility.

Let us now consider the reasons for the variation of the orientability, λ, and the molded mechanical properties with the rate of elongation. Attention will be focused on the results for $\alpha = 6°$, d = 3/8", 40 v/o of 1/8" fibers, given in Figures 5 and 6. There are three different regimes of flow to be considered:

i) low $\dot{\varepsilon}_{11}$ ($< 0.36\ sec^{-1}$), where λ and E increase with increasing elongation rate

ii) moderate $\dot{\varepsilon}_{11}$ ($0.36 < \dot{\varepsilon}_{11} < 10\ sec^{-1}$) where λ and E decrease with increasing elongation rate

iii) high $\dot{\varepsilon}_{11}$ ($> 10\ sec^{-1}$), where an abrupt increase in E is observed.

The flow behavior in these regions is influenced by the granular structure of the molding compound, as well as the high voidage, which causes the material to be inhomogeneous.

Only the molding compounds made from 1/8" or longer fibers at a high loading, 40 v/o, demonstrate the anomalous dependence of orientation on elongation rate. These materials in the noncompacted condition consist of well-defined grains, each consisting of numerous fiber bundles held tightly together with a thin coating of resin. The structure during fill for a highly expanded material is shown in Figure 17. When shorter fibers or a lower fiber loading (excess resin) are employed, such distinct grains do not form.

At very low flow rates, Takano [14] and Hagan and Thomas [15] have observed that the flow of a concentrated fiber suspension through a small orifice may be intermittent. Although this may not actually occur in the wider channels of our experiments, the slow flows are thought to be locally nonuniform. The meshing together of the granular units as the cross-sectional area is reduced will cause an alternating movement between different regions of the cross-section. Secondary flows may also occur. The resulting swirled and oscillatory orientation patterns cause not only a strong local fluctuation in the measured angle ϕ_3 over small distances, but also reduce the distance-averaged orientation parameter λ.

In regime i), as the elongation rate increases up to the optimum value of 0.36 sec^{-1}, the flow becomes smoother because the higher orienting stress can more easily overcome the flow

resistance of the grains. At the same time, the void content is increasing slightly.

Beyond the maximum point and into regime ii), it is believed that λ is reduced by hydrodynamic instabilities in the flow that become significant only at the higher elongation rates. Some typical oscillations of the planar angle ϕ_3 measured in the cone are shown in Figure 18. The scale of these oscillations is much larger than the grain size shown previously in Figure 17. Since the elongation rate increases rapidly near the cone exit, and since a discontinuity in the streamline direction also exists at the cone-to-rod juncture, the instabilities are probably more severe at that point and limit the orientation in the rod to the 20° range, regardless of the degree of orientation predicted from the λ values. The occurrence of wild oscillations at the rod entrance and their continued existence, though at a reduced amplitude, into the rod is shown in Figure 19.

In the first two orientation regimes, then, the orientation in the rod is controlled by the size of the orientation parameter, λ, which itself is hypothesized to depend on flow disturbances of two types. On the other hand, the third regime, which is defined by $\bar{\varepsilon}_{11} > 10.\ \mathrm{sec}^{-1}$ is characterized by a sharp increase in the rod stiffness that is not accompanied by a corresponding increase in the measured λ, but rather by a decrease in the local angle fluctuations. The increase in smoothness of the flow is dramatically shown by a comparison of the two axial orientation profiles in a 22-1/2° cone measured above and below the critical

$\bar{\varepsilon}_{11}$ for transition to the third regime, in parts a and b of Figure 18. The high rod rigidity at a relatively low average λ for the cone is possible through a sharp local increase in λ in the very high elongational strain rate that exists near the cone exit. The behavior is illustrated in Figure 20. It occurs only at very high local rates of strain (> about 60. sec^{-1}) and is accompanied by a smooth and stable orientation pattern. Rod properties in this regime are controlled by conditions at the cone-rod junction rather than by the overall orientation behavior in the cone.

One could hypothesize that the critical elongation rate for entrance into regime iii) corresponds to the point at which the fiber network fractures, thus relieving built-up elastic stresses that tend to resist orientation change. This conjecture is supported by the absence of a maximum point in the λ and mechanical property data for milled fibers. Such short fibers would not be capable of forming an interpenetrating network that could sustain an elastic force. Consequently, the memory of these materials is nonexistant, oscillatory orientation patterns do not occur, and the orientation continues to improve, though slowly, into better axial alignment as $\bar{\varepsilon}_{11}$ increases. However, the flow of the milled glass suspensions is complicated because their lower structure may also allow substantial shear to occur.

For the 90° entrance angle, regimes ii and iii overlap. It has been shown that a very high elongation rate is required to enter iii. A change in the elongation rate at the same flow rate and 90° geometry can be due to a movement of the natural channel boundary that separates the flowing portion from the stagnant region at the corners. Visual observation of polished sections of the entrance region show that the higher stiffness of the upper-branch in Figure 9 is associated with smaller oscillations in the rod, especially at the centerline, and that these, in turn, occur when the stagnant region is smaller. Periodic plugging of the rod entrance would also be a likely flow disturbance when $\alpha = 90°$, particularly for the smallest diameter rod.

The orientation and consequent mechanical properties in molded rods thus depend upon two causative phenomena. These are the average rate of orientation change in the converging section preceding the rod, which can be correlated with the average rate of elongational strain in that section, and entrance effects at the cone - rod juncture. The latter depend upon the locally high elongation rate there and are associated with a sharp increase in the smoothness of the axial orientation profiles. This decrease in the short-range variations of orientation is probably a requisite for the enhanced rigidity observed in regime iii).

Conclusions and Summary.

When a polymer containing a high concentration of moderately long ($\geq$ 1/8") discontinuous fibers flows into an empty cavity the porosity is high (> 10%) and the orientability parameter, λ, in the equation

$$\left(\frac{\tan \theta_1}{\tan \theta_1^\circ} \right) = \frac{A}{A^\circ}^{\frac{3}{2}\lambda}$$

is not a constant but depends on the rate of elongation in an extensional flow. At the optimum rate of elongation λ takes on a maximum value of 1.16. High voidage results from an upstream diverging channel, such as would be produced by a small gate. If no such region exists above a converging channel, λ might be expected to be a constant, equivalent to that obtained in flow under a compaction pressure (4).

In that case, a relatively low value of .47 results for λ, because the mobility of the fibers is more restricted. Mobility is increased in suspensions of lower fiber content, because of less severe fiber interaction. It increases to .63 at 20 v/o. Reducing the fiber length might also be expected to lead to a lower interaction. However, λ is reduced if the fibers are too short ($\leq$ 1/32"), because the hydrodynamic forces causing the rotation cannot act as effectively. On the other hand, increasing fiber length from 1/8" to 1/4" causes a decrease in the maximum λ for low density flows from 1.16 to 0.86. The bending and tangling of the longer fibers inhibits their rotation. 1/8" is the optimum fiber length.

The highest degree of longitudinal orientation that can be obtained in a practical elongational flow of 1/8" or longer fibers in an epoxy matrix is characterized by an average angle of 20°. However, this represents a significant improvement over conventional molding practice, wherein an end-gated part contains a central core of transverse fiber orientation. Tensile strength can be increased more than threefold from 7,000 to 27,000 psi and modulus from 1.5 to 3.9 x 10^6 psi by instituting the proper control of orientation.

The limitations on orientability, λ, and on the actual orientation distribution produced in a rod molded through a converging section are hypothesized to result from inhomogeneous movement and fiber blocking at low flow or elongation rates, and from flow instabilities at moderately high rates. When the elongation rate exceeds about 60. sec^{-1}, the flow experiences a sharp transition into a smooth state. Under this condition, λ increases and the established orientation pattern remains undisturbed in the molded rod.

This transition may correspond to the point of material fracture, above which the elastic stresses in the fiber network resisting orientation change are destroyed. The relaxation of these elastic stresses would cause the oscillations observed in the orientation pattern in the rods molded at rates below the transition. At very low elongation rates the stresses would be permitted to relax during the flow, permitting the high value of λ at the optimum rate of 0.36 sec^{-1}.

It might be possible to mold a fiber-reinforced thermoplastic resin by such a combination of cooling rate and flow that the orientations are frozen before the fiber network can relax, yielding a more perfect alignment than was possible in this work.

Acknowledgment

The author wishes to express his gratitude to Mr. D. J. Morotz and to Miss A. M. Gordon for their assistance in the experimental phases of this study.

This research was supported by the Advanced Research Projects Agency of the Department of Defense and was monitored by the Office of Naval Research under contract no. N00014-67-C-0218.

REFERENCES

1. Takserman-Krozer, R., and A. Ziabicki, J. Polymer Sci., A1, 491 (1963).

2. Ericksen, J. L., Kolloid Z., 173(2), 117 (1960).

3. Bell, J. P., J. Composite Mat., 3, 244 (1969).

4. Goettler, L. A., Monsanto/Washington Univ. ONR/ARPA Assoc. Report HPC 70-130.

5. Goettler, L. A., Monsanto/Washington Univ. ONR/ARPA Assoc. Report HPC 72-149; also SPE Antec 1973, p. 559.

6. Stankoi, G. G., E. B. Trostyanskaya, Y. N. Kazanskii, V. V. Okorokov and O.Y. Mikhasenok, Soviet Plastics, Sept. 1968, p. 47.

7. Hoffman, K. R. and E. R. Fiala, SPE Antec, March 1966.

8. Hoffman, K. R. and J. W. Vellturo, Polymer Tech., 16(8), 50 (Aug. 1970).

9. Andersen, H. M. and D. C. Morris, 23rd Annual SPI Reinforced Plastics/Composites Division Tech. Conference, 1968.

10. Goettler, L. A., Modern Plastics, 48, 140 (April 1970).

11. Takano, M., Monsanto/Washington University ONR/ARPA Report HPC 68-73, AD 849285, Feb. 1969.

12. Goettler, L. A., unpublished data.

13. Bagg, G. E. G., L. E. Dingle, H. Edwards, M. E. N. Evans and H. Ziebland, 7th International Reinforced Plastics Conference, London, Oct. 1970, p. 6/1.

14. Takano, M., to be published.

15. Thomas, D. P. and R. S. Hagan, 21st SPI Reinforced Plastics Division Meeting, 1966, Section 3-C.

16. Lavengood, R. E., private communication.

17. Goettler, L. A., Monsanto/Washington Univ. ONR/ARPA Assoc. Report HPC 72-151.

LIST OF FIGURES

1. Channel geometry; D = 1.25"; d = .25, .375, or .50 inches.

2. Elongation rate effects in the determination of λ; 40 v/o 1/4" CS308 fiberglass, $\alpha = 6°$, d = 3/8".

3. Elongation rate variations in a 6° cone.

4. A comparison of actual and extrapolated orientation angles to investigate a possible wall effect; 40 v/o 1/4" CS308 fiberglass, $\alpha = 6°$.

5. Elongation rate effects on the orientability parameter, λ; 40 v/o 1/8" CS308A fiberglass, d = 3/8".

6. Rate effects on the predicted and measured rod stiffness; 40 v/o 1/8" CS308A fiberglass, d = 3/8" (A°/A = 11.1).

7. Relationship of rod stiffness to measured average polar angle, $\bar{\theta}_1$, for various 1/8" fiberglass/epoxy transfer moldings (5).

8. Viscosity levels in the transfer moldings of 3/8" rods; 40 v/o 1/8" CS308A fiberglass, $\alpha = 6°$.

9. Stiffness in 3/8" rods molded through a 90° entrance angle; 40 v/o 1/8" CS308A fiberglass.

10. Ultimate tensile strength in 3/8" rods molded through a 90° entrance angle; 40 v/o 1/8" CS308A fiberglass.

11. Stiffness in 1/4" molded rods; A°/A = 25.0, $\alpha = 6°$, 40 v/o 1/8" CS308A fiberglass.

12. Stiffness in 1/2" molded rods; A°/A = 6.25, $\alpha = 6°$, 40 v/o 1/8" CS308A fiberglass.

13. Orientability parameter, λ, for longer 1/4" fibers, 47 v/o 1/4" CS308, $\alpha = 6°$, d = 3/8".

14. Tensile properties of 1/2" rods molded from 1/4" fibers; $\alpha = 6°$, 41 v/o 1/4" CS308A.

15. Orientation parameter and molded rod stiffness for milled glass fiber; 44 v/o 1/32" OCF Type 701B, $\alpha = 6°$, A°/A = 11.1 (3/8" rod).

16. Typical cross-section of a molding of .5 mil dia. glass fibers in epoxy.

17. Grains in a non-compacted molding compound flowing into an empty mold cavity.

18. Oscillation in the axial orientation profile in the cone; α = 22-1/2°, d = 3/8", 40 v/o 1/8" fiberglass; a: $\dot{\bar{\varepsilon}}_{11} = 6.7\ \mathrm{sec}^{-1}$; b: $\dot{\bar{\varepsilon}}_{11} = 19.4\ \mathrm{sec}^{-1}$.

19. Oscillations in the axial orientation profile extending into the rod; α = 90°, d = 3/8", Q = 28.4 in^3/min; 40 v/o 1/8" fiberglass.

20. Increase in λ with smoothness of flow near the cone exit; α = 22-1/2°, 40 v/o 1/8" fiberglass, d = 3/8", $\dot{\bar{\varepsilon}}_{11} = 19.4\ \mathrm{sec}^{-1}$.

LIST OF TABLES

1. Limiting and average elongation rates in conical channels.

2. Agreement of rod stiffness for 3/8" moldings made at high flow rate through a 90° entrance with predictions from λ.

3. Variation of stiffness with rod diameter with a 90° entrance; 40 v/o 1/8" CS308A fiberglass.

4. Discrepancy between attained orientation and that predicted from λ values.

5. Comparison of measured mechanical properties with those based on λ values.

6. Effect of bundle aspect ratio.

7. Summary of tensile properties of molded composite rods.

8. Comparison of methods for aligning fibers.

TABLE 1

Limiting and Average Elongation Rates

Angle degrees	Rod dia. inches	$X_{1,out}$ inches	$X_{1,in}$ inches	$\frac{\dot{\varepsilon}_{11}}{Q}$, $\frac{min}{in^3\text{-}sec}$ In	Avg	Out
6	1/4	1.189	5.95	.0092	.138	1.151
	3/8	1.784	5.95	.0092	.0665	.341
	1/2	2.379	5.95	.0092	.0402	.1438
22-1/2	1/4	.302	1.51	.040	.600	5.06
	3/8	.453	1.51	.040	.289	1.50
	1/2	.604	1.51	.040	.175	0.63

TABLE 2

Agreement of rod stiffness for 3/8" diameter molding made at high flow rate through a 90° entrance with predictions from λ

Q	$\bar{\dot{\varepsilon}}_{11}$	$E \times 10^{-6}$	$E_{pred} \times 10^{-6}$	%
in^3/min	sec^{-1}	psi	psi	difference
2.47	3.68	2.52	2.65	+4.9
4.46	6.65	2.33	2.30	-1.3
24.1	35.9	1.90	2.00	+5.0

TABLE 3

Effect of Area Reduction Ratio when $\alpha = 90°$

A^o/A	Rod Diameter inches	Q in^3/min	$E \pm \sigma_M$ $\times 10^{-6}$ psi	$E - E_{3/8"}$ $\times 10^{-6}$ psi	σ_u 10^3 psi
25.	1/4	3.1	2.31 ± .11	-.17	23.2
11.1	3/8	3.1	2.48		12.6
11.1	3/8 (upper branch)	19.0	2.62	+.05	26.5
6.25	1/2	19.0	2.67 ± .01		22.0

TABLE 4

Discrepancy of Attained Orientation from λ-Prediction

$\alpha = 6°$ 1/8" JMCS308A Fiberglass

40 v/o

Rod diameter inches	$\frac{A°}{A}$	At $\bar{\varepsilon}_{11}$* Predicted $\bar{\theta}_1$, degrees	At $\bar{\varepsilon}_{11}$* Actual θ_1, degrees	At $\bar{\dot{\varepsilon}}_{11} = 1.\ sec^{-1}$ Predicted $\bar{\theta}_1$, degrees	At $\bar{\dot{\varepsilon}}_{11} = 1.\ sec^{-1}$ Actual $\bar{\theta}_1$, degrees
1/2	6.25	10.1	22.5	32.4	29.5
3/8	11.1	3.8	20.8	19.1	21.2
1/4	25.	0.9	22.2	8.4	25.7

TABLE 5

Discrepancy of Measured Rod Stiffness from λ Prediction

$$\bar{\dot{\epsilon}}_{11} = 1.0 \text{ sec}^{-1}$$

Rod diameter inches	A°/A	Predicted E x 10^{-6}, psi	Actual E x 10^{-6}, psi	% deviation	Actual Tensile Strength x 10^{-3}, psi
1/2	6.25	2.38	2.57	- 8	16.0
3/8	11.1	3.85	3.39	+ 12	26.6
1/4	25.	4.45	2.82	+ 37	21.0

TABLE 6

Effect of Bundle Aspect Ratio

Rod diameter = 3/8" Fiber length = 1/4"

$\alpha = 6°$

Fiber designation	# of filaments per strand	Fiber content v/o	E x 10^{-6} psi	Tensile strength x 10^{-3}, psi	Average tensile elongation, %
CS308	120	47	3.12 ± 0.40	24.4 ± 2.1	.98
CS308A	240	44 47*	3.12 ± 0.19 3.32*	27.6 ± 2.1	1.11

*corrected according to the volume fraction rule, assuming a fiber efficiency of 85%.

TABLE 7

Summary of Tensile Properties of Molded Composite Rods

$\dot{\varepsilon}_{11}$ sec^{-1}	Rod diameter	A°/A	40 v/o $\alpha = 6°$ Tensile Modulus, 10^6 psi Fiber length 1/4"	1/8"	≤ 1/32"	Tensile strength, 10^3 psi Fiber length 1/4"	1/8"	≤ 1/32"
	1/2"	6.25	2.55	1.90	-	7.0	-	-
3.6	3/8"	11.1	2.86	2.48	2.12*	27.6*	19.4	9.0*
	1/4"	25.	3.15	2.66	-	31.9	19.4	-
0.36	1/2"	6.25	3.27	3.13	-	18.4	17.5	-
(optimum)	3/8"	11.1	2.86	3.57	1.72*	27.6*	27.1	8.0*
	1/4"	25.	-	3.18	-	-	22.3	-

* 44 v/o

TABLE 8

Comparison of Methods for Aligning Short Fibers

Glass fibers in an epoxy matrix

Process	Ref.	Fiber content v/o	Average Fiber angle $\bar{\theta}_1$, degrees	E 10^6 psi	Tensile strength 10^3 psi
Controlled transfer molding	this work	40	19	3.9	27.
Extrudate lay-up	(9)	40 57	20 20	3.5 5.0	33. 35.
Conventional transfer molding	(10)	40	40-60	1.5	7.
Couette flow encapsulation + lay-up	(11)	57	7.	5.7	45.
Elongated grain lay-up	(12)	70	14.	7.0	39.
E.R.D.E. process	(13)	57*	-	14.	57. (ref. 16) (ranged 43. to 73. with 1" gauge length)

*graphite fiber, Modmor Type II

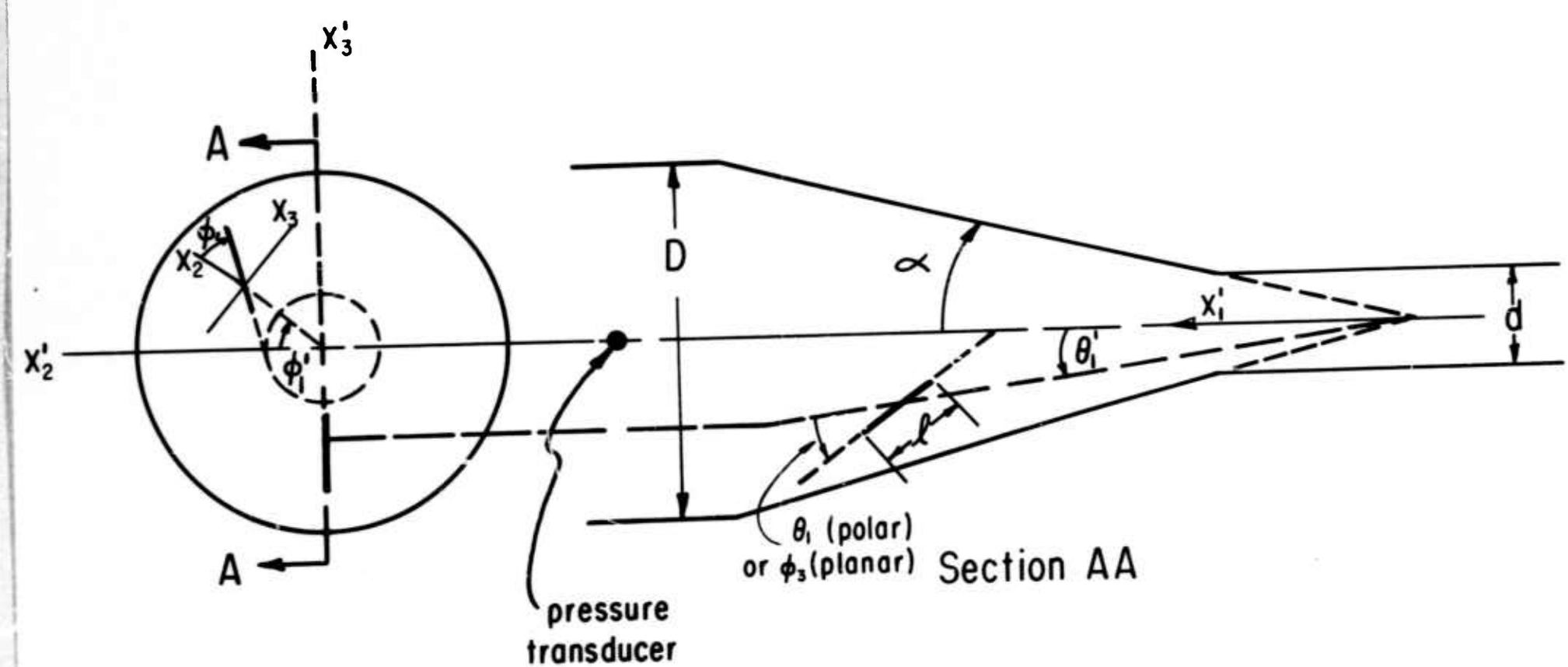

1. Channel geometry; D = 1.25 inches, d = .25; .375, or .50 inches.

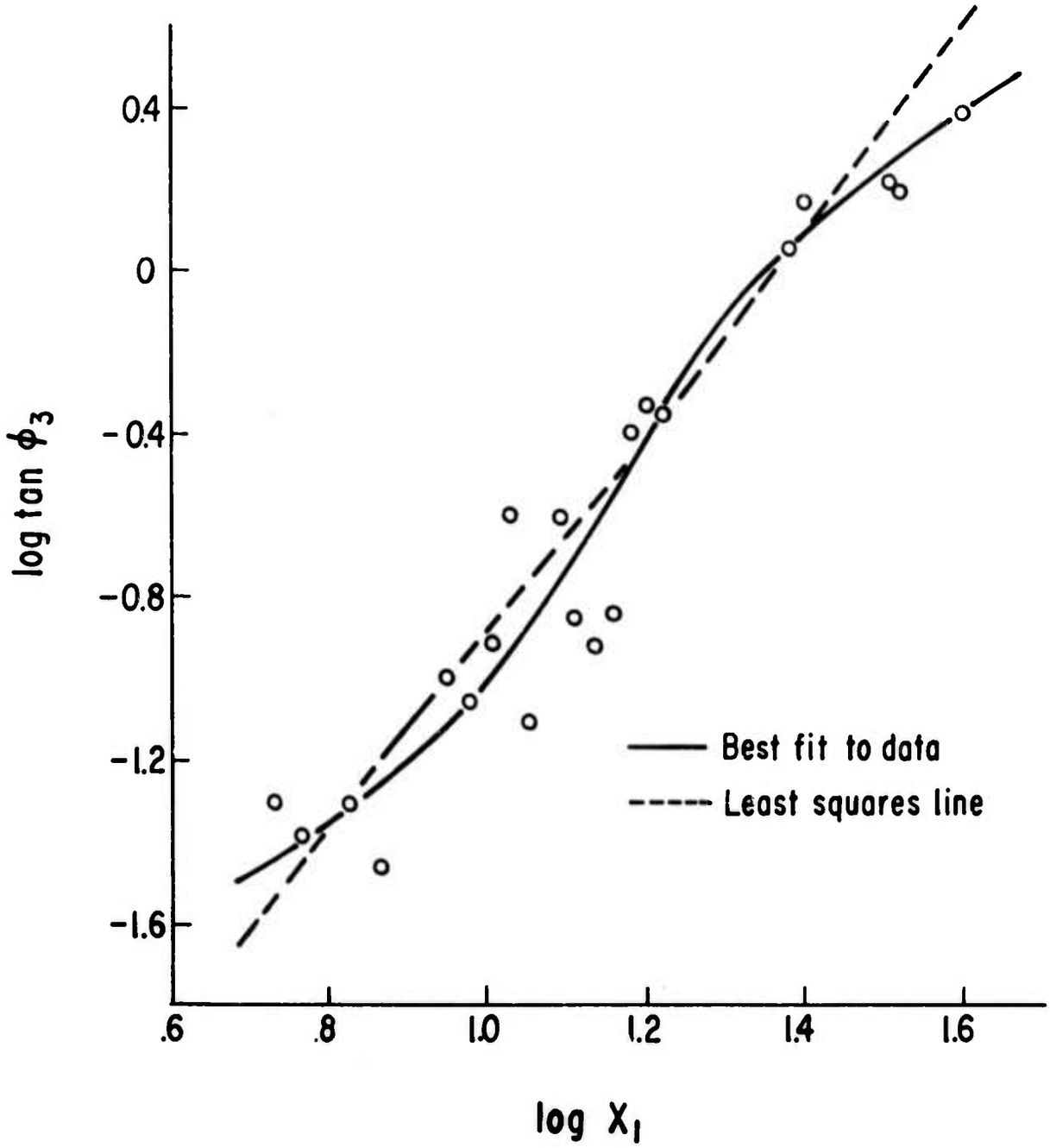

2. Elongation rate effects in the determination of λ; 40 v/o 1/4" CS308 fiberglass, $\alpha = 6°$, d = 3/8".

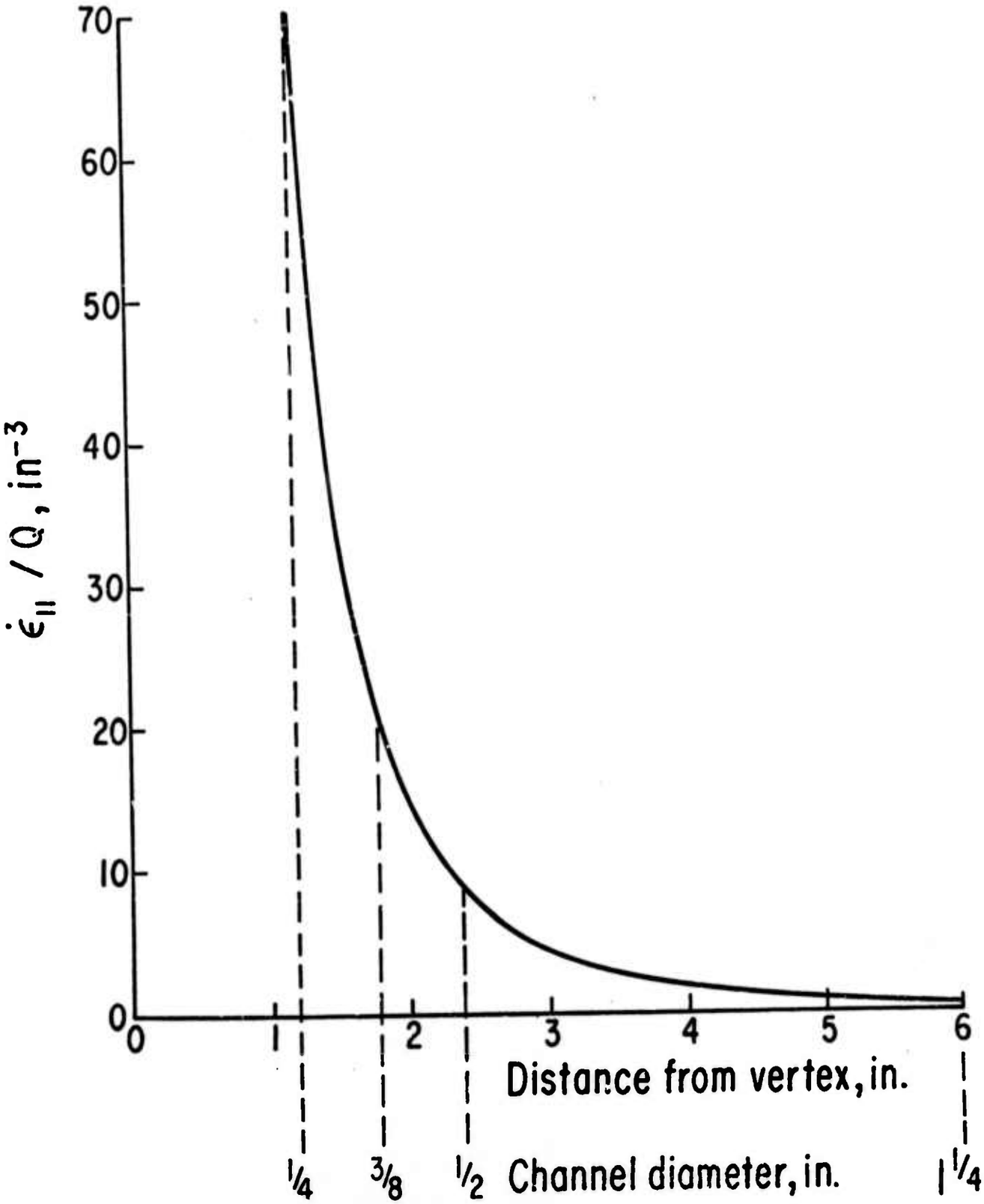

3. Elongation rate variations in a 6° cone.

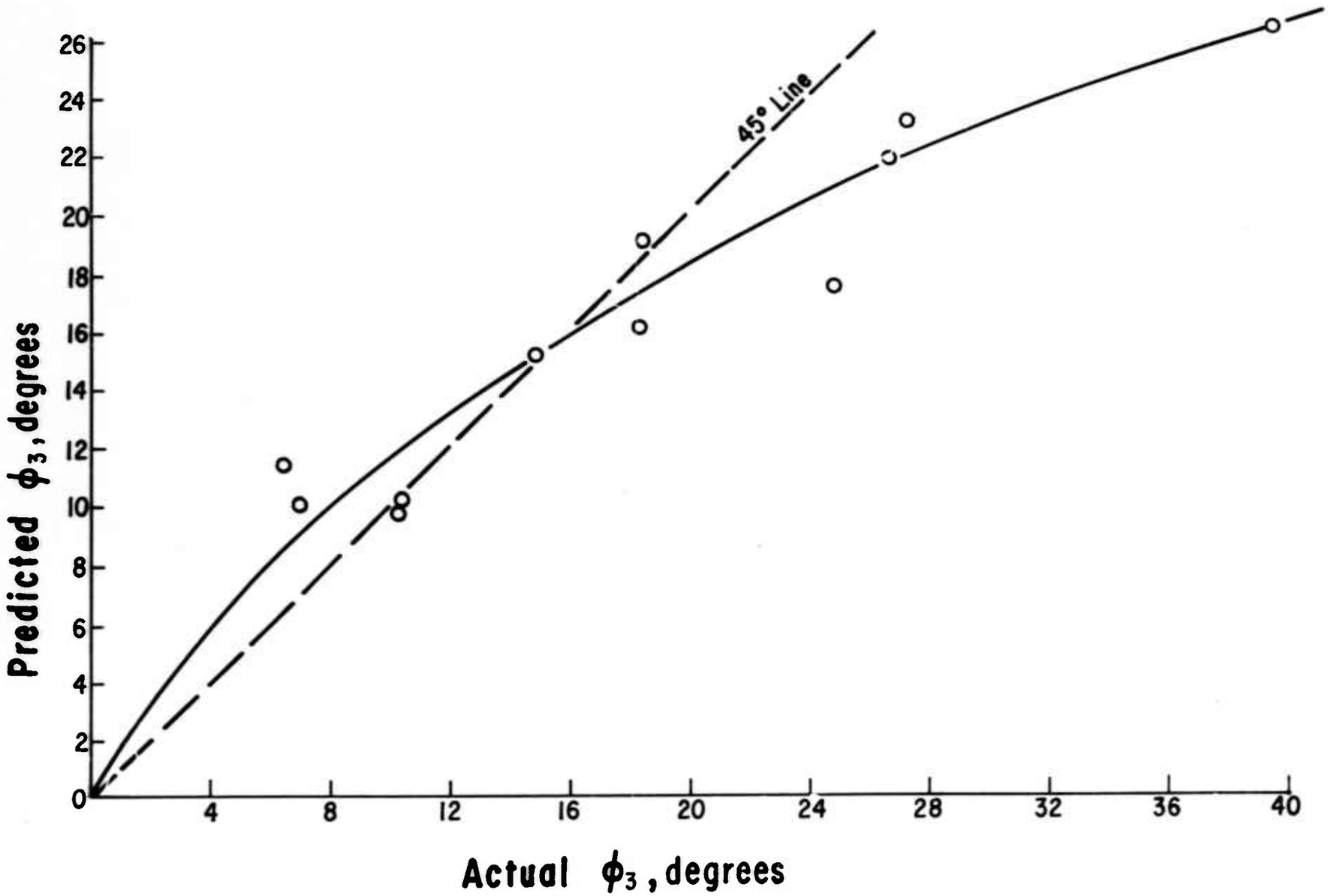

4. A comparison to actual and extrapolated orientation angles to investigate a possible wall effect; 40 v/o 1/4" CS308 fiberglass, $\alpha = 6°$.

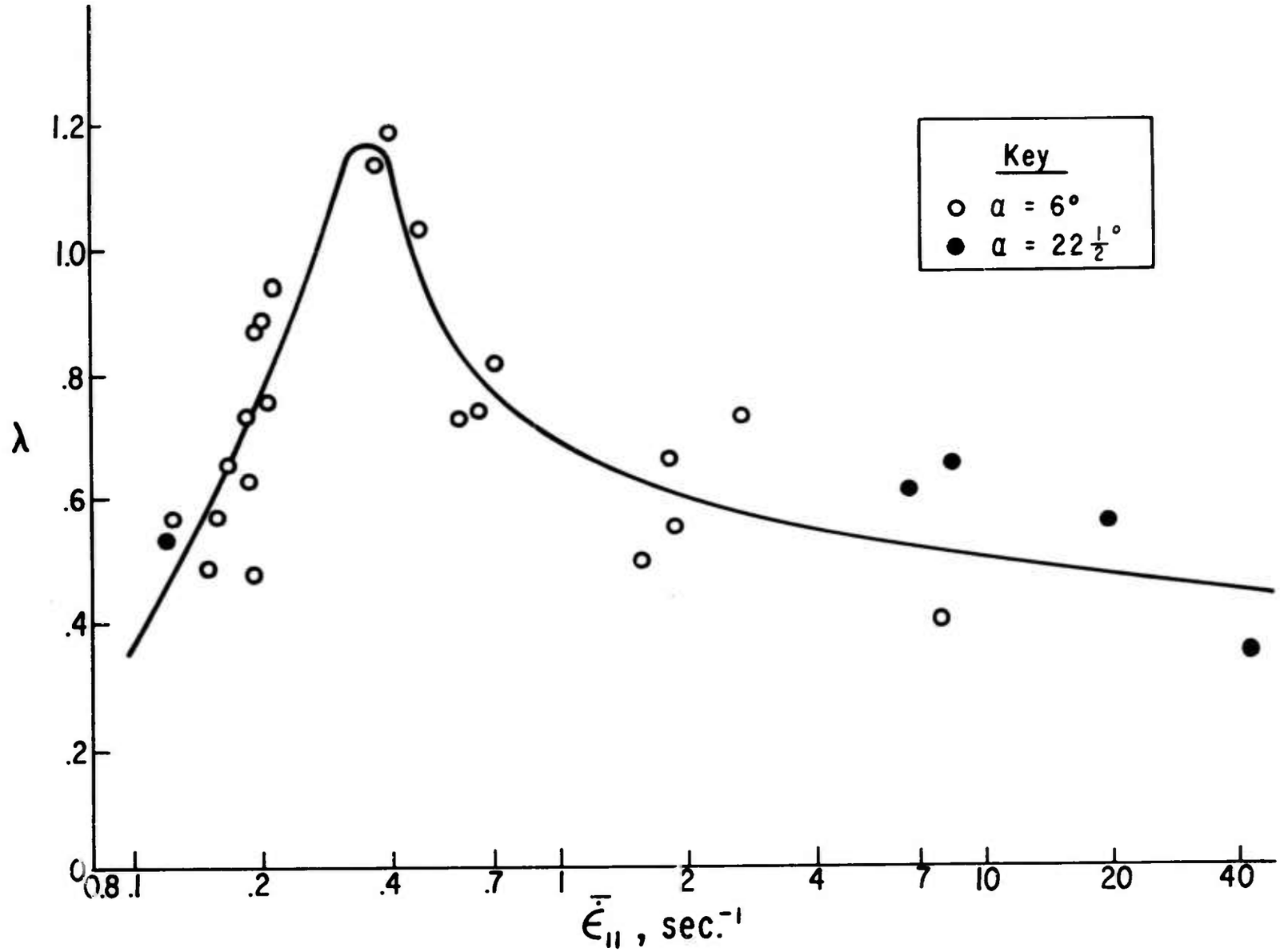

5. Elongation rate effects on the orientability parameter, λ; 40 v/o 1/8" CS308A fiberglass, d - 3/8".

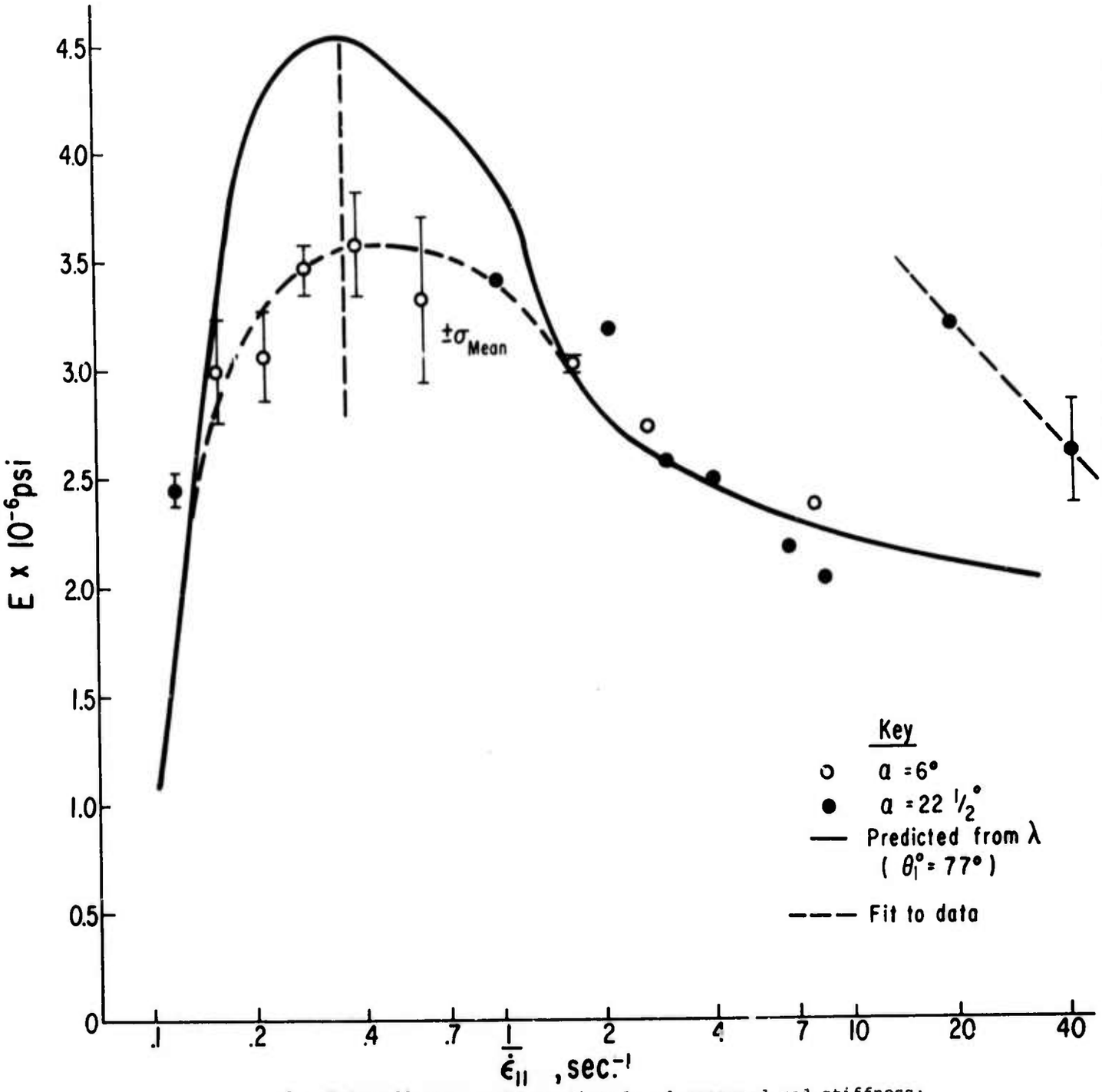

6. Rate effects on the predicted and measured rod stiffness; 40 v/o 1/8" CS308A fiberglass, d - 3/8" (A°/A = 11.1).

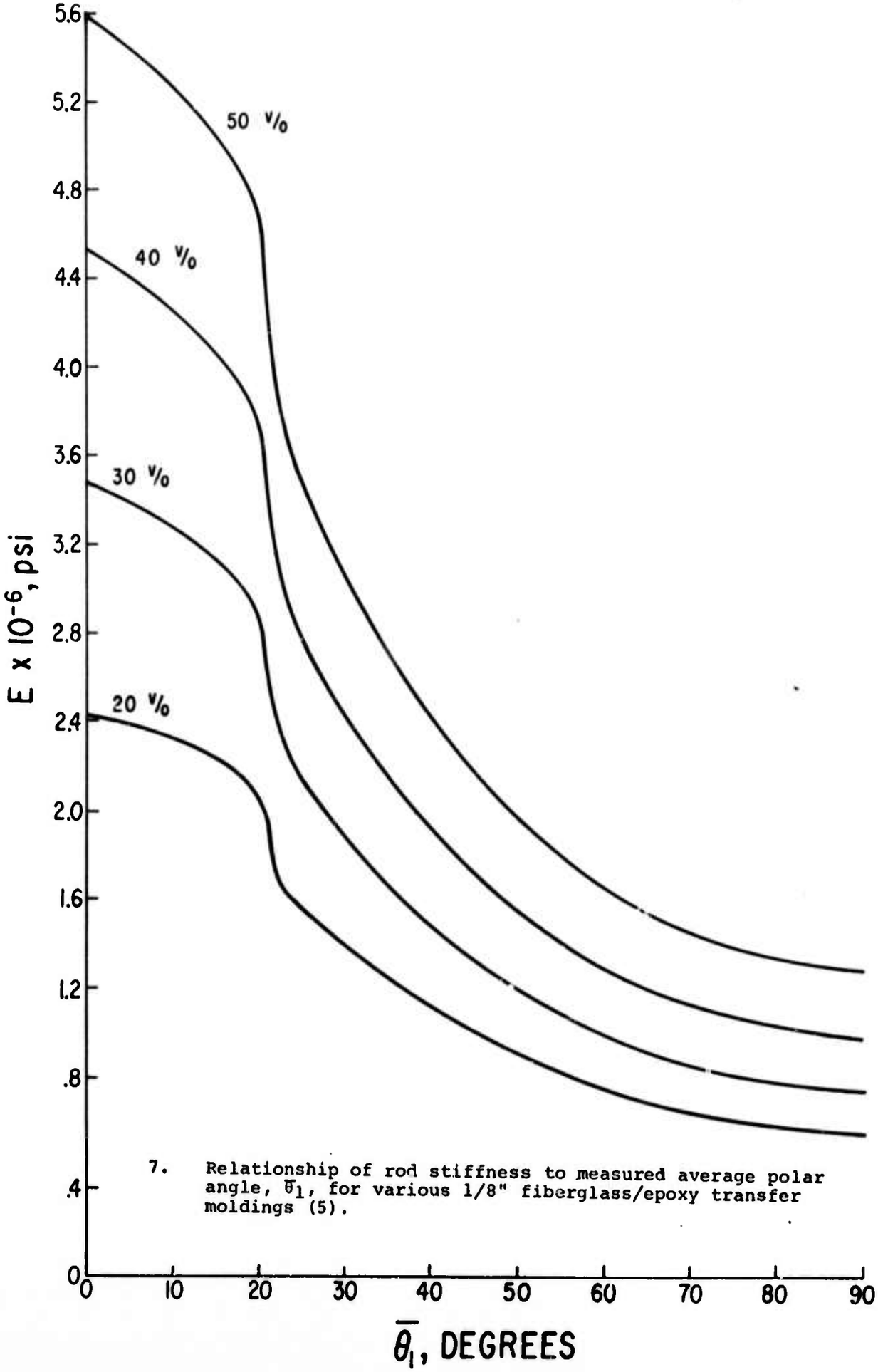

7. Relationship of rod stiffness to measured average polar angle, $\bar{\theta}_1$, for various 1/8" fiberglass/epoxy transfer moldings (5).

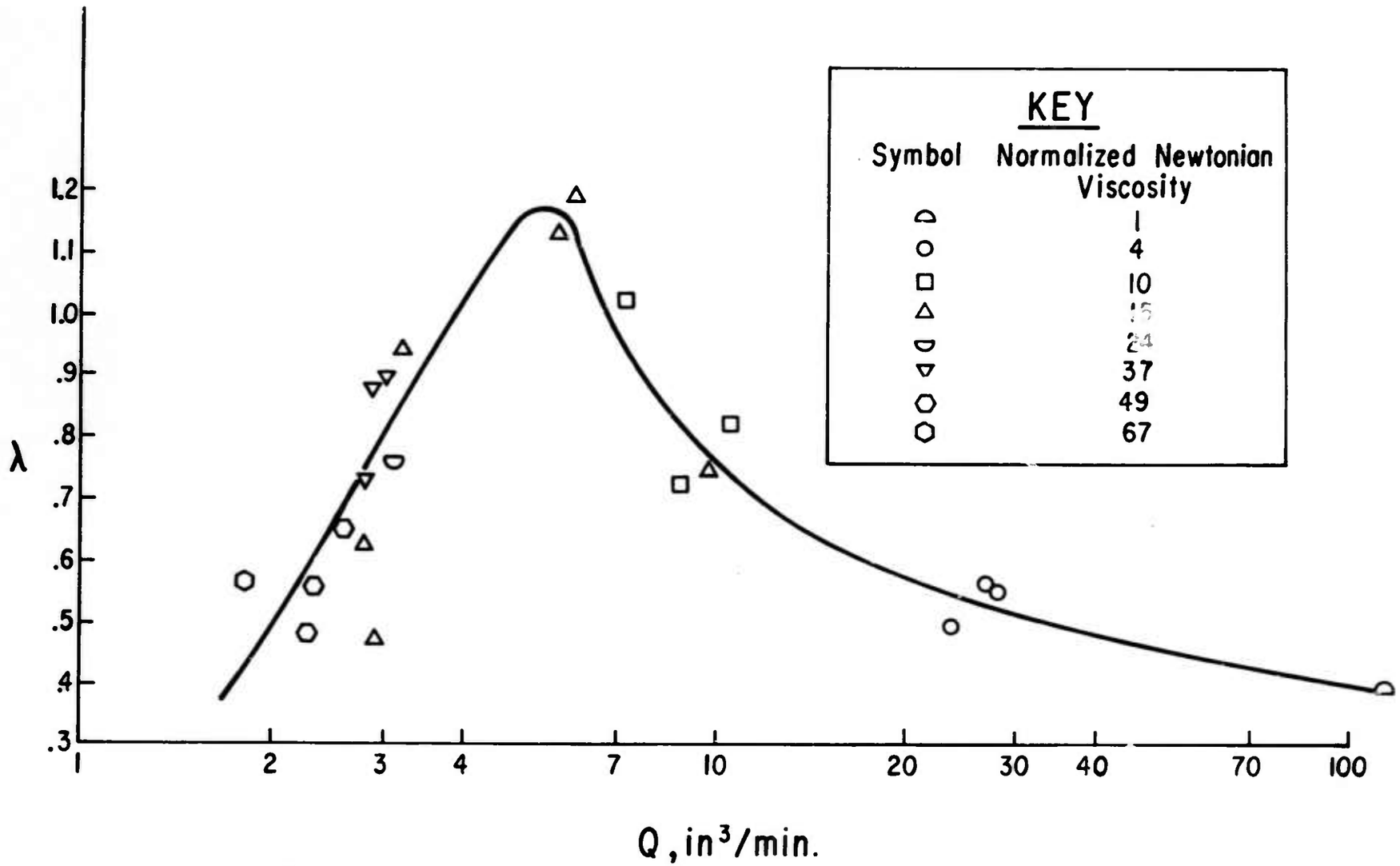

8. Viscosity levels in the transfer moldings of 3/8" rods; 40 v/o 1/8" CS308A fiberglass, $\alpha = 6°$.

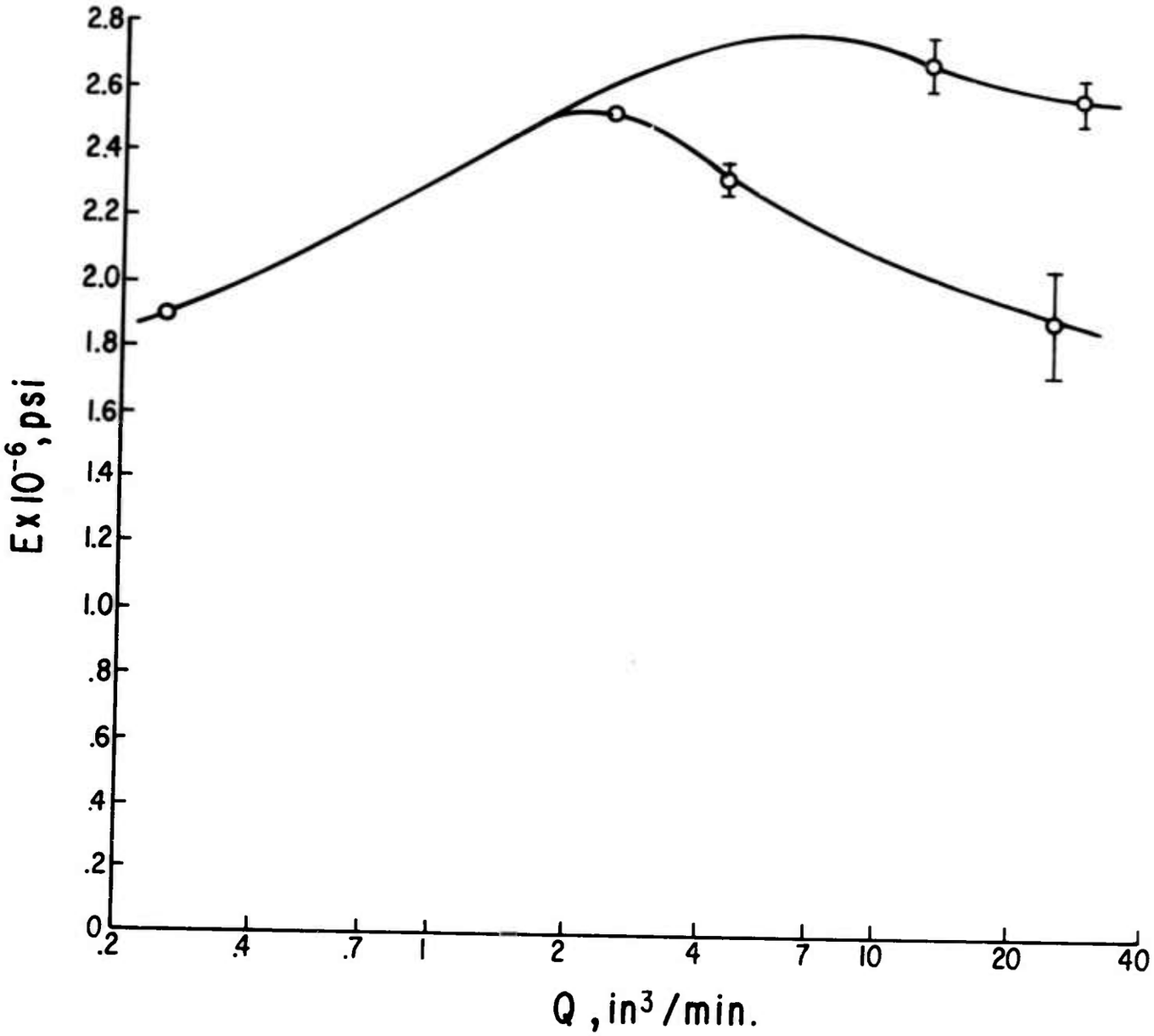

9. Stiffness in 3/8" rods molded through a 90" entrance angle; 40 v/o 1/8" CS308A fiberglass.

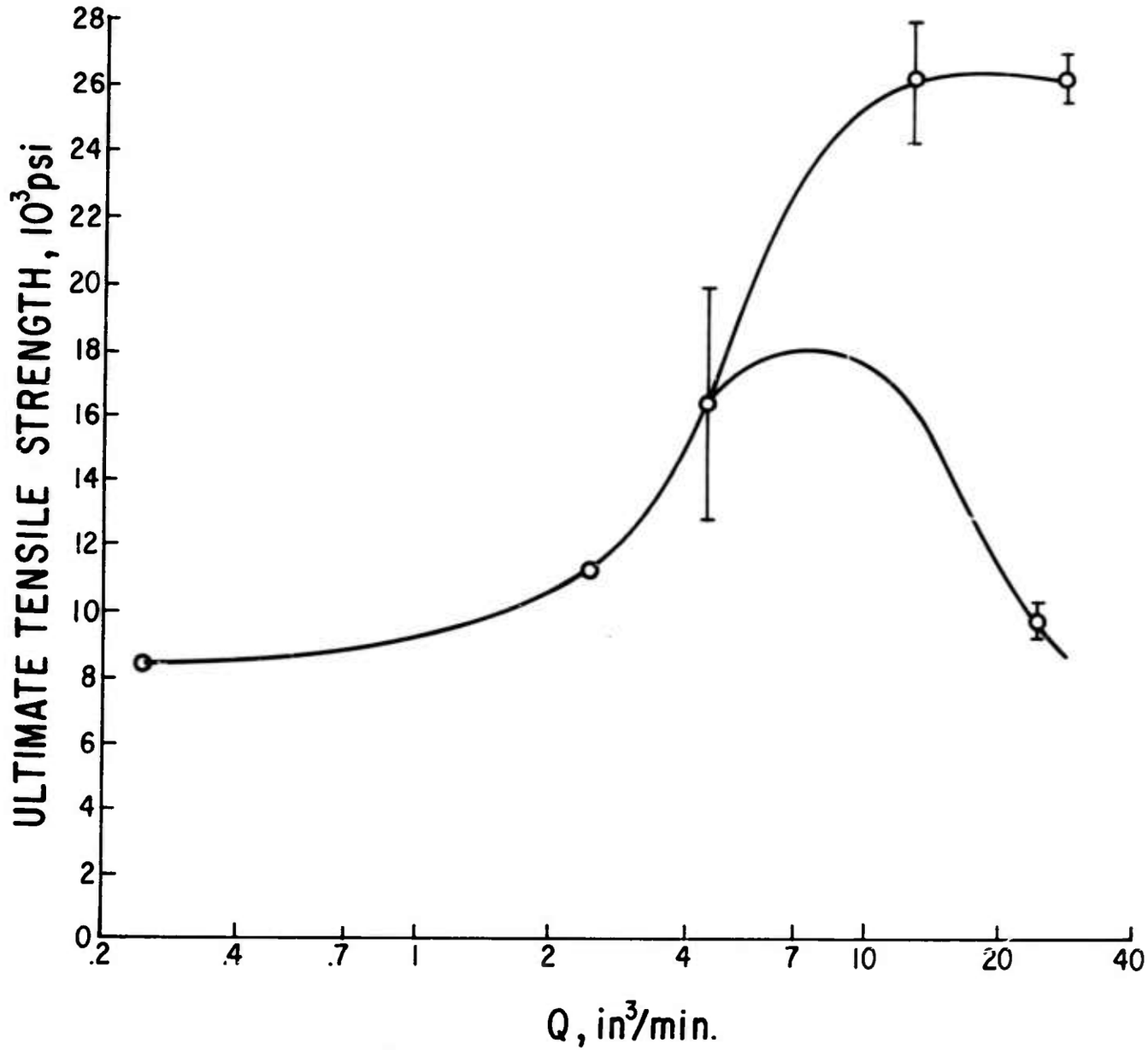

10. Ultimate tensile strength in 3/8" rods molded through a 90° entrance angle; 40 v/o 1/8" CS308A fiberglass.

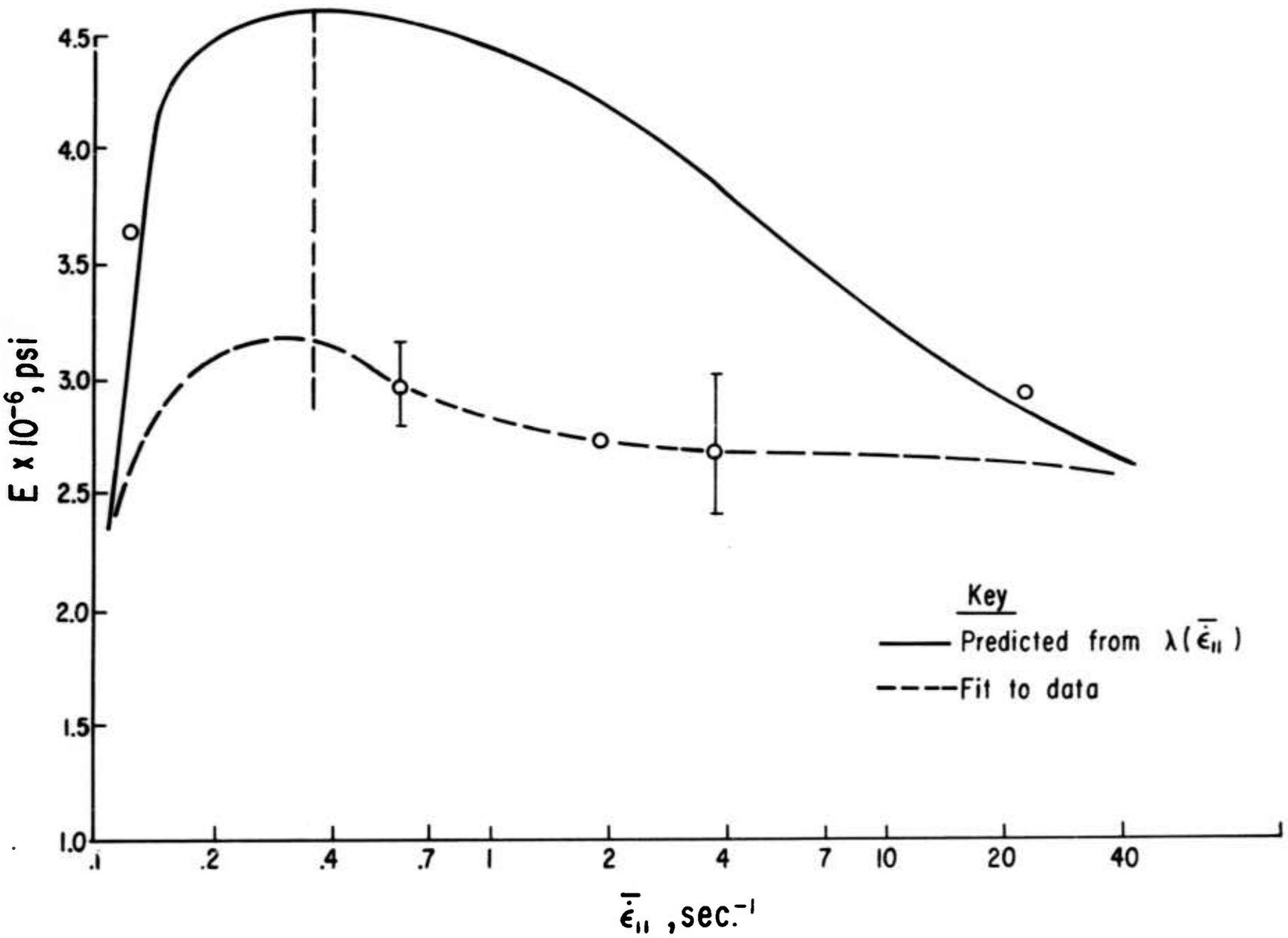

11. Stiffness in 1/4" molded rods; $A^{\circ}/A = 25.0$, $\alpha = 6^{\circ}$, 40 v/o 1/8" CS308A fiberglass.

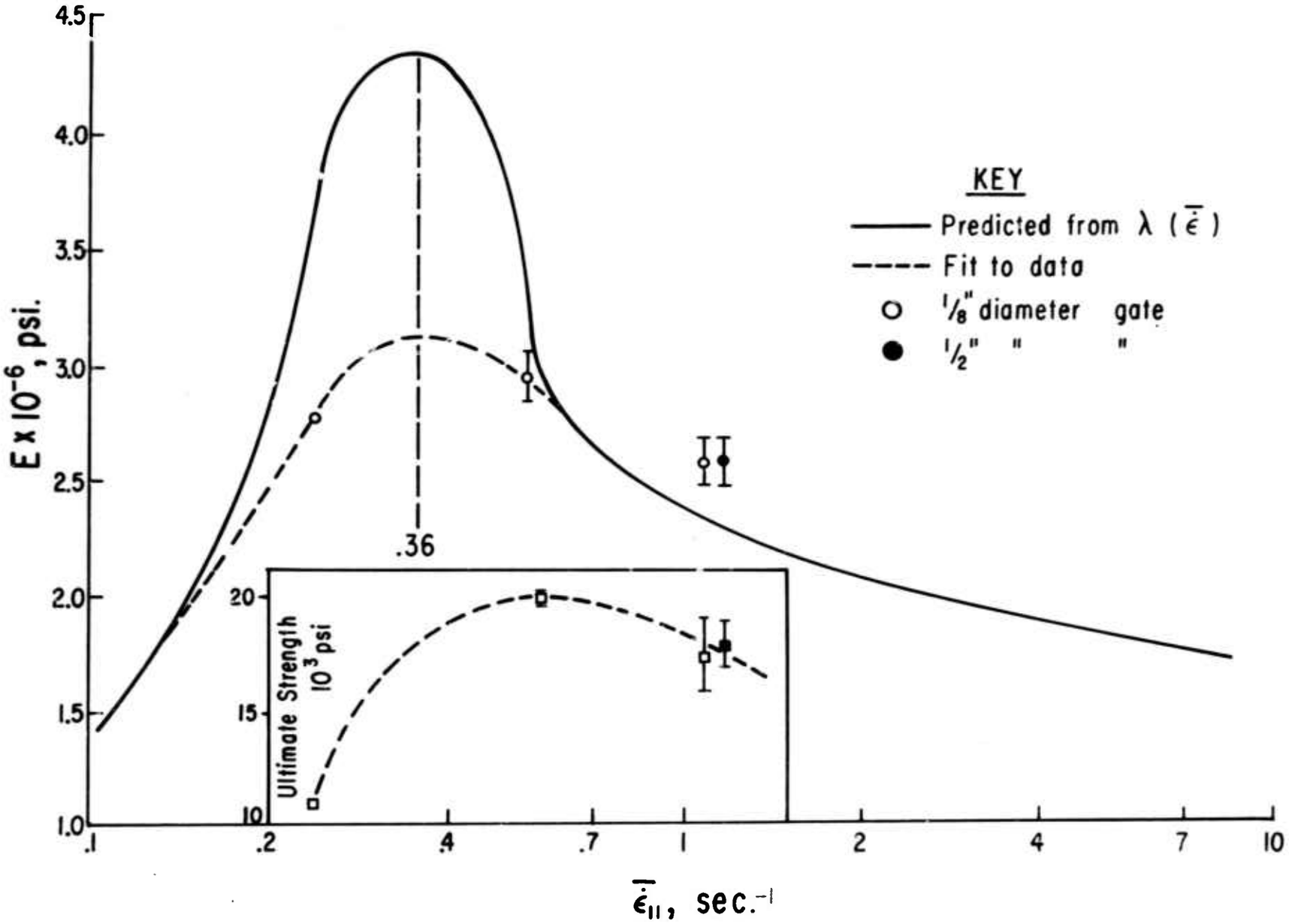

12. Stiffness in 1/2" molded rods; $A^{\circ}/A = 6.25$, $\alpha = 6^{\circ}$, 40 v/o 1/8" CS308A fiberglass.

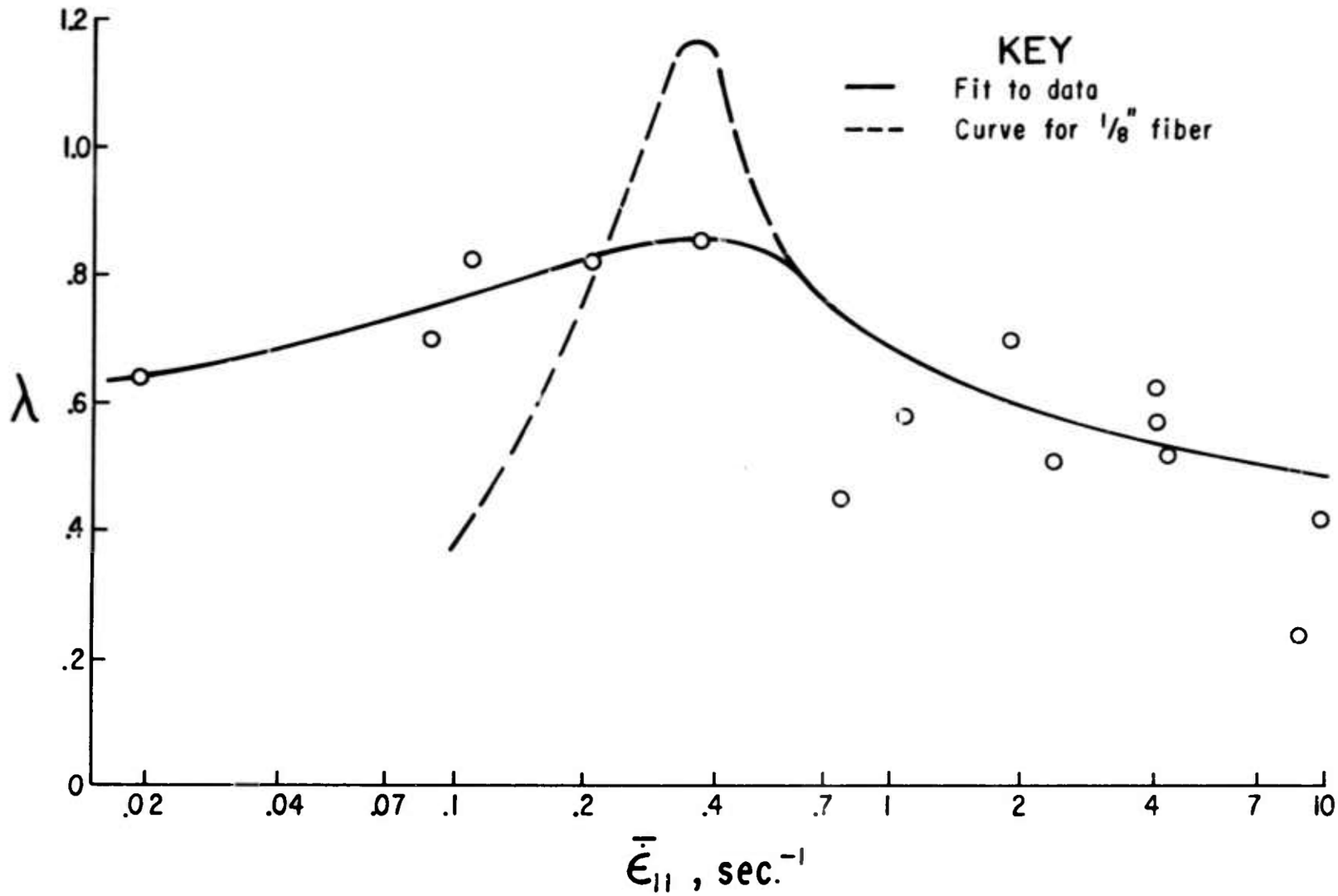

13. Orientability parameter, λ, for longer 1/4" fibers, 47 v/o 1/4" CS308, α = 6°, d = 3/8".

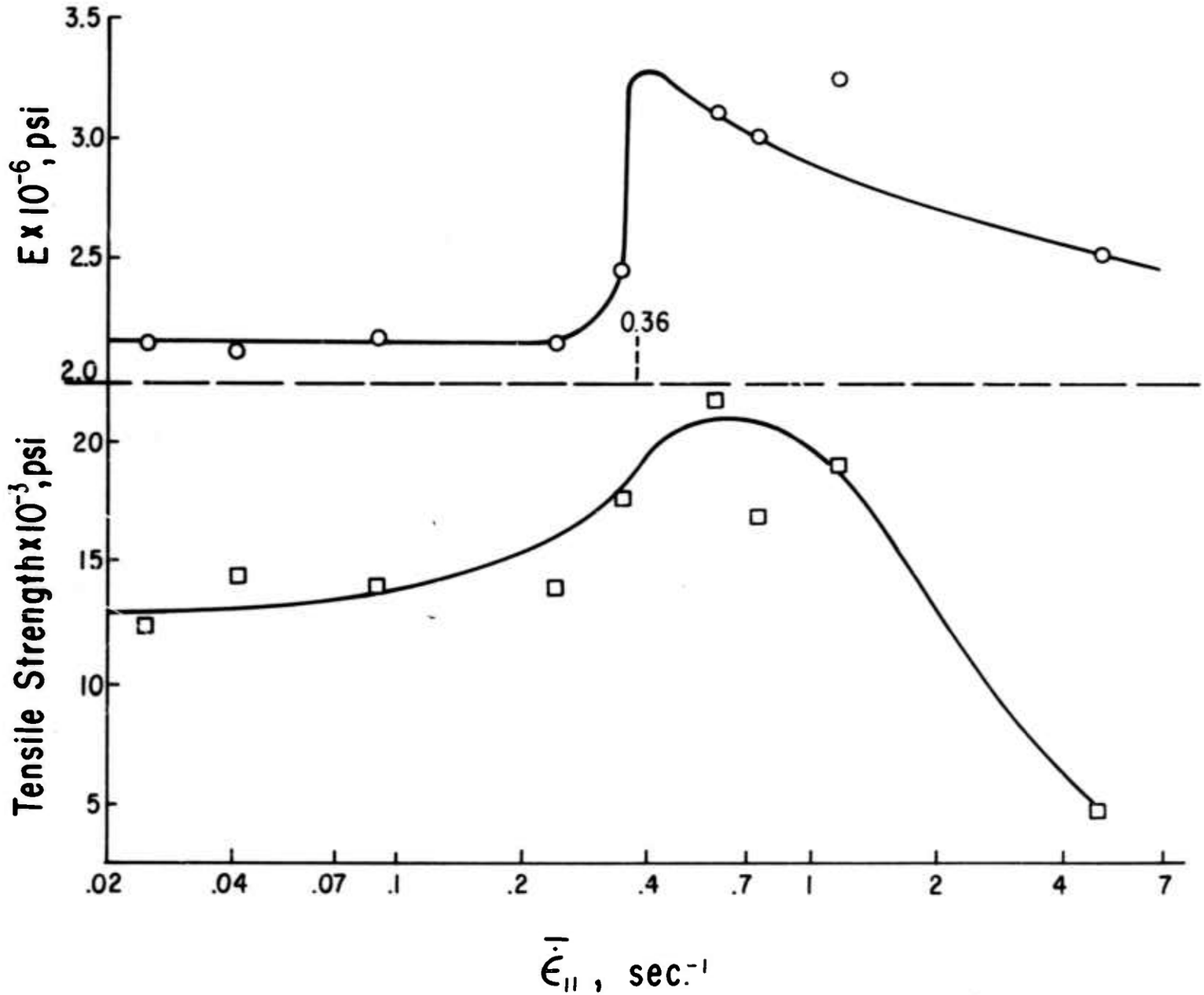

14. Tensile properties of 1/2" rods molded from 1/4" fibers; $\alpha = 6°$, 41 v/o 1/4" CS308A.

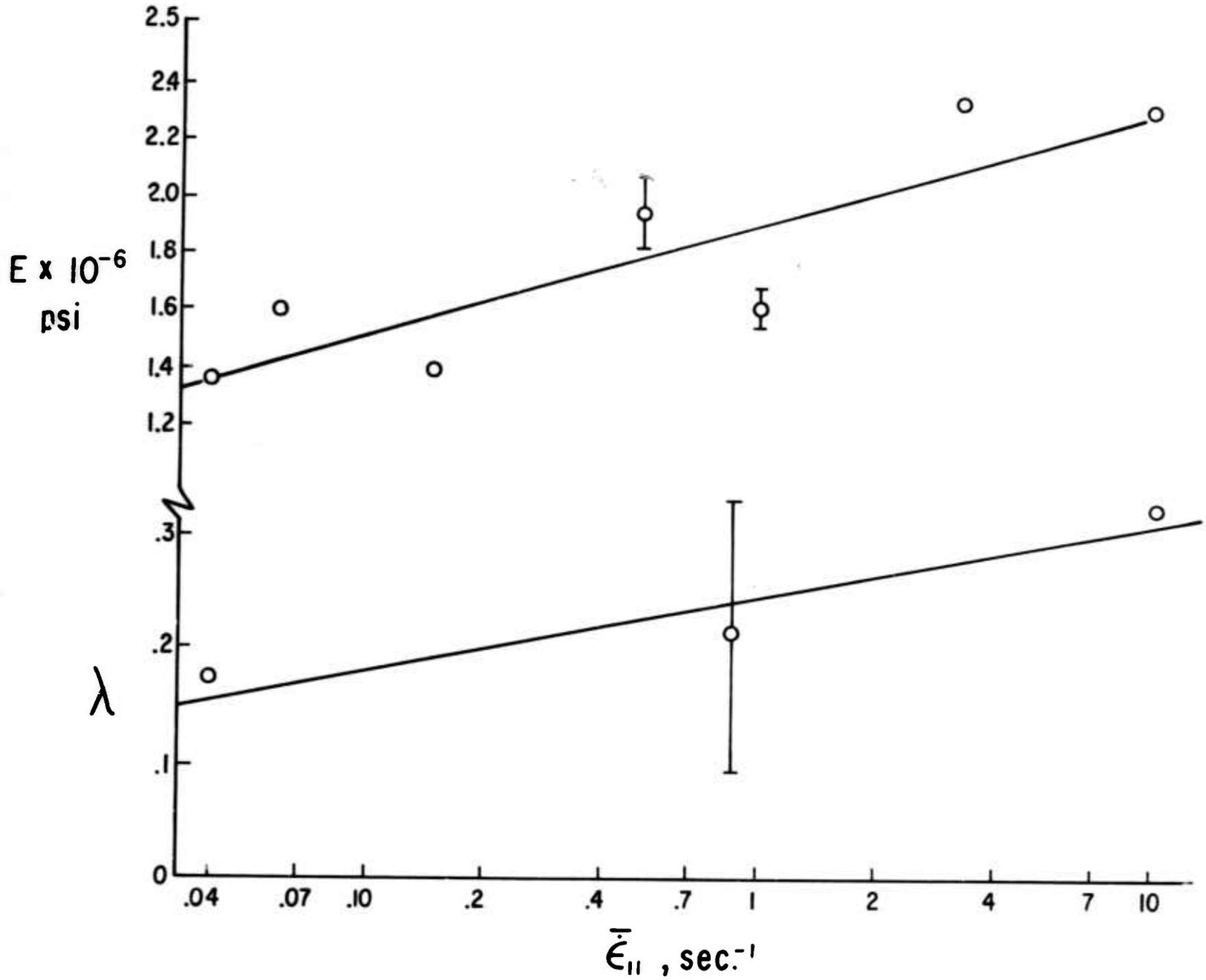

15. Orientation parameter and molded rod stiffness for milled glass fiber; 44 v/o 1/32" OCF Type 701B, $\alpha = 6°$, $A°/A = 11.1$ (3/8" rod).

Reproduced from best available copy.

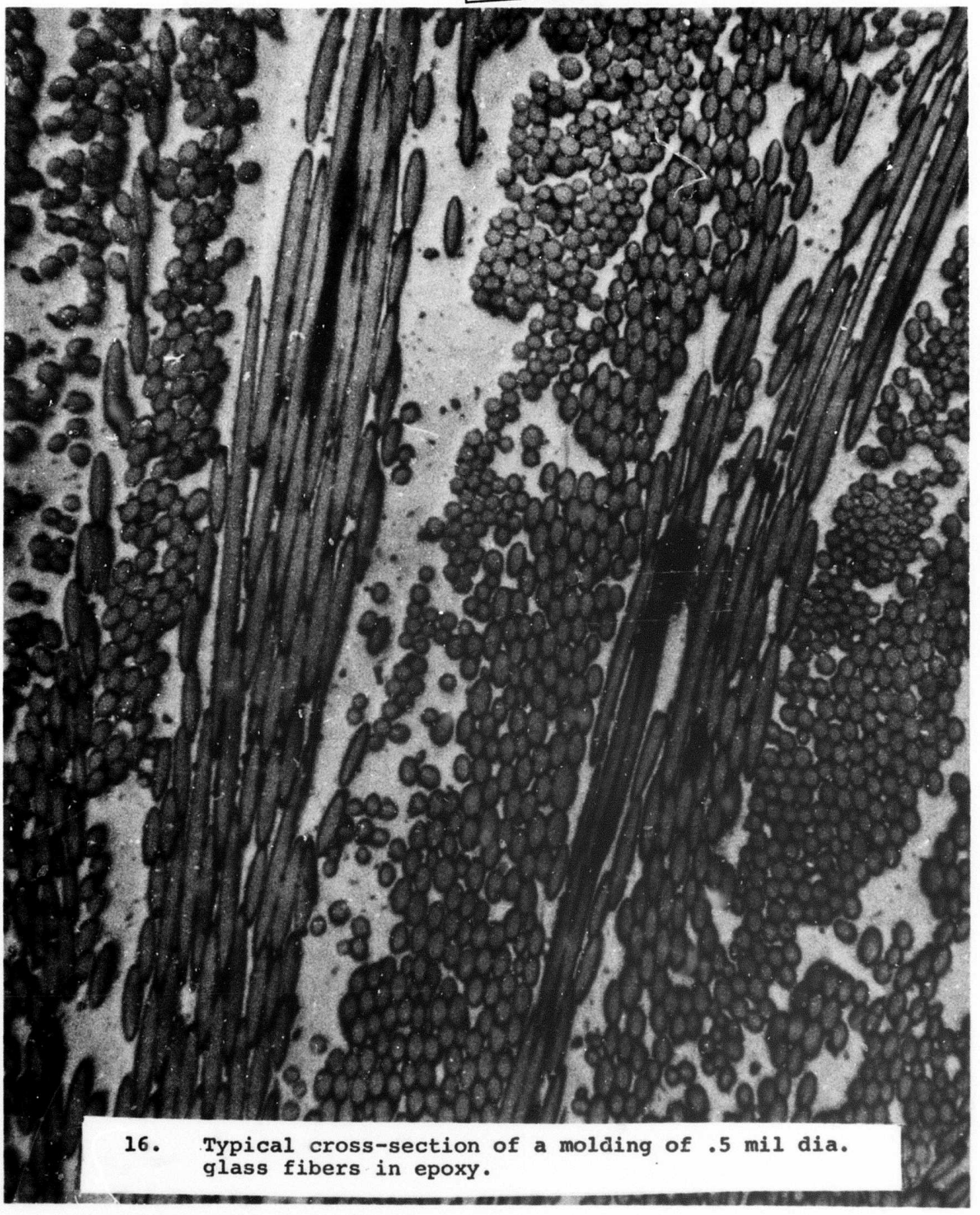

16. Typical cross-section of a molding of .5 mil dia. glass fibers in epoxy.

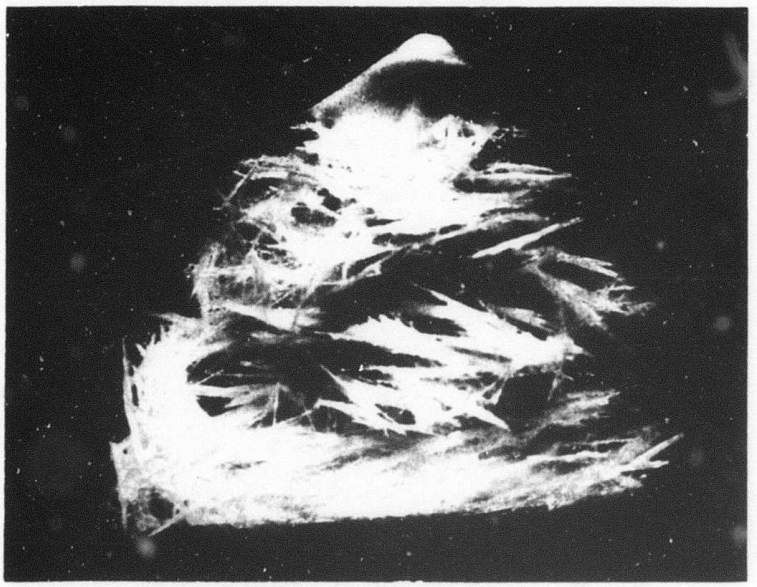

17. Grains in a non-compacted molding compound flowing into an empty mold cavity.

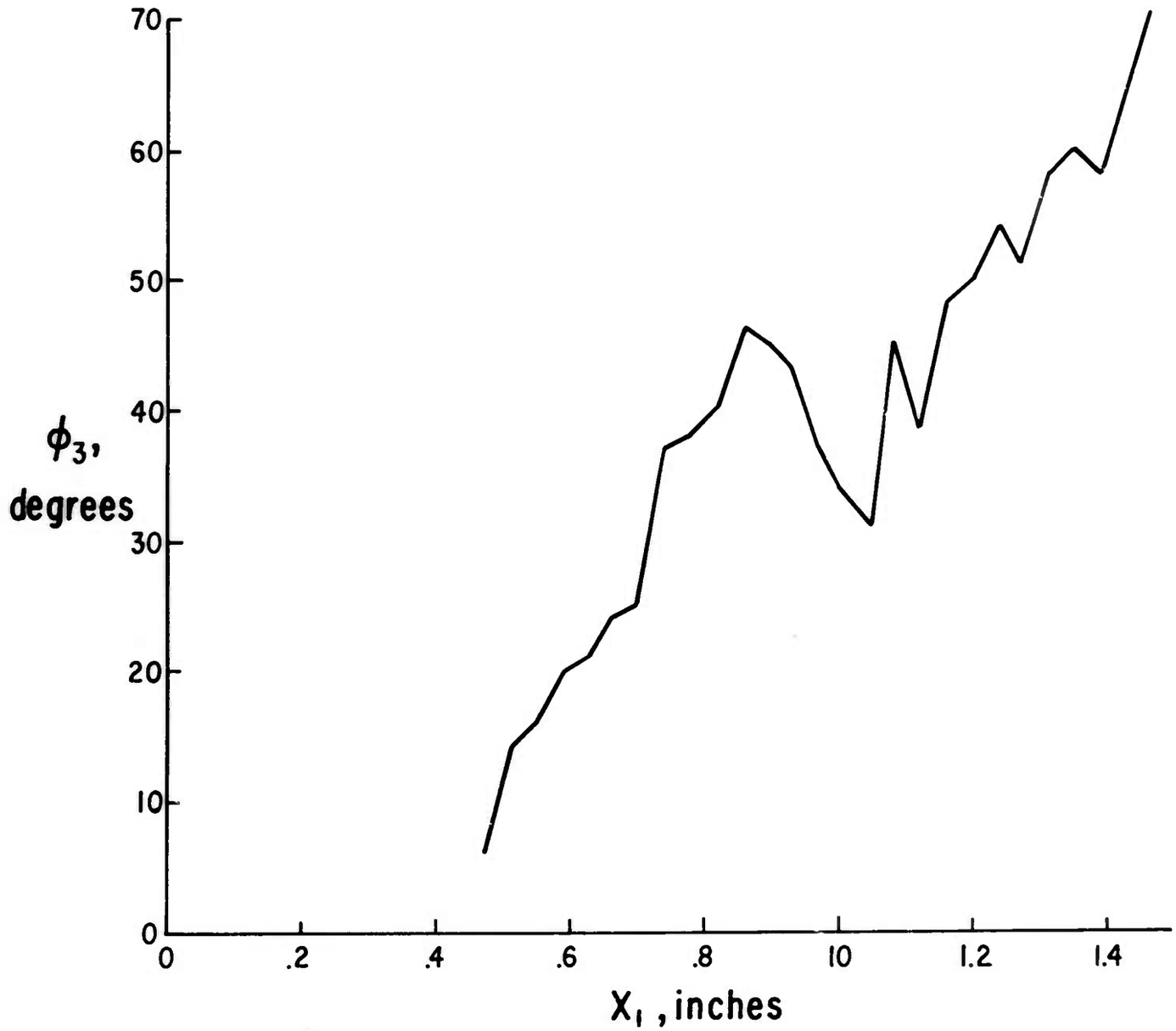

18b. Oscillation in the axial orientation profile in the cone; $\alpha = 22\text{-}1/2°$, d = 3/8", 40 v/o 1/8" fiberglass; b: $\dot{\bar{\varepsilon}}_{11} = 19.4\ \text{sec}^{-1}$.

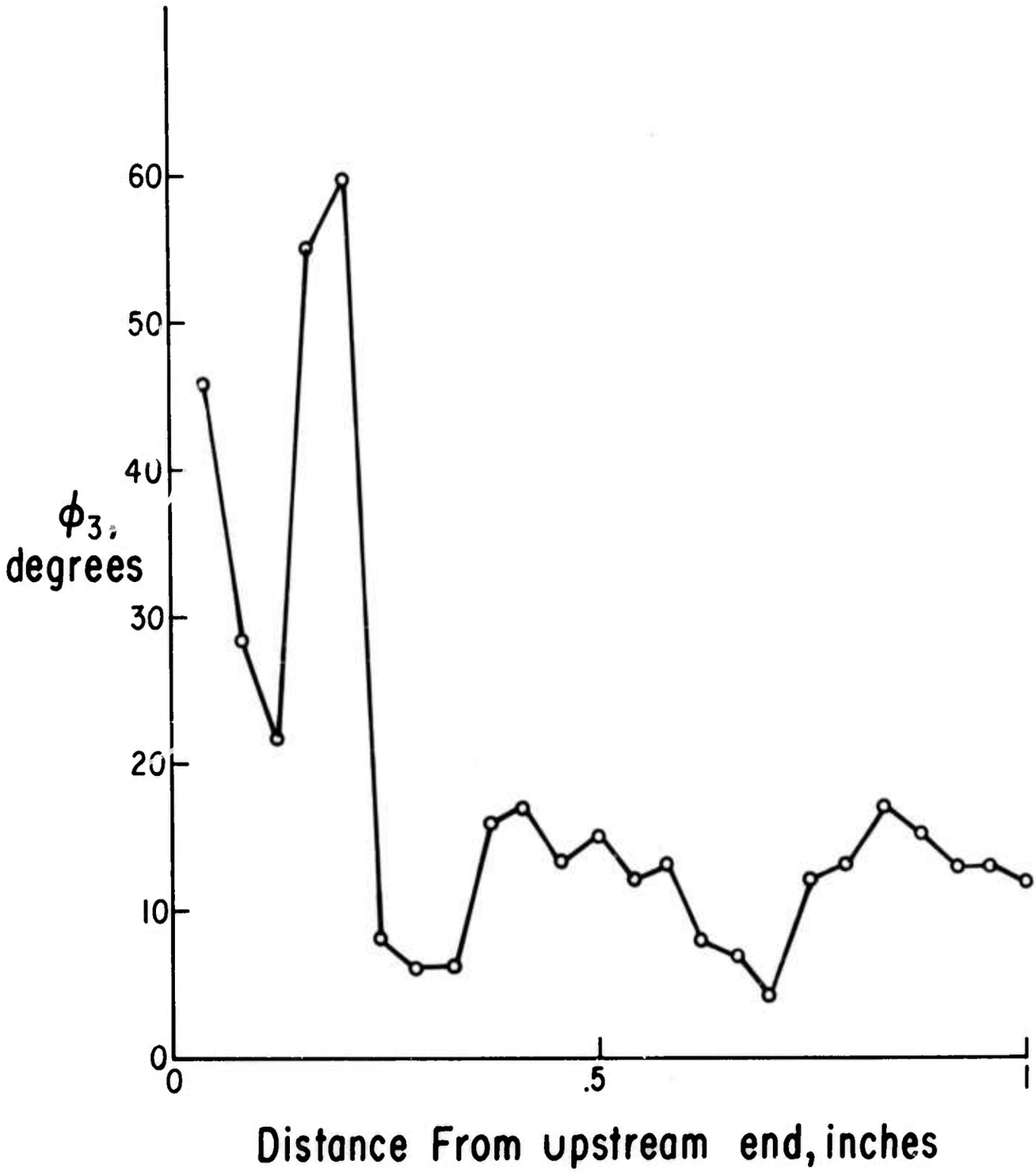

19. Oscillations in the axial orientation profile extending into the rod; $\alpha = 90°$, d = 3/8", Q = 28.4 in^3/min; 40 v/o 1/8" fiberglass.

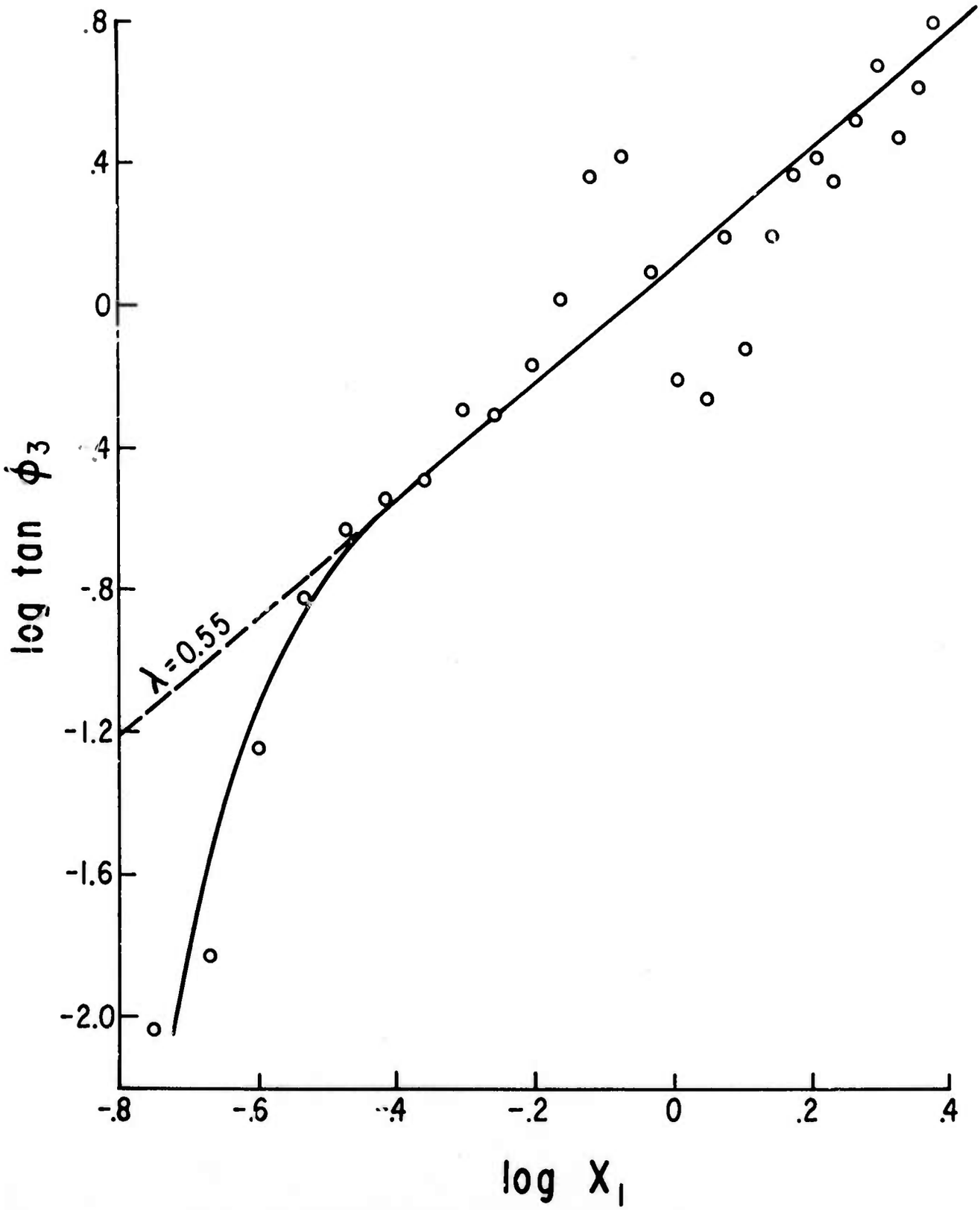

20. Increase in λ with smoothness of flow near the cone exit; α = 22-1/2°, 40 v/o 1/8" fiberglass, d = 3/8", $\bar{\varepsilon}_{11}$ = 19.4 sec^{-1}.